

## Bora wind characteristics for engineering applications

Petra Lepri<sup>1</sup>, Željko Večenaj<sup>2</sup>, Hrvoje Kozmar<sup>\*3</sup> and Branko Grisogono<sup>2</sup>

<sup>1</sup>Meteorological and Hydrological Service, Grič 3, 10000 Zagreb, Croatia

<sup>2</sup>Department of Geophysics, Faculty of Science, University of Zagreb,  
Horvatovac 95, 10000 Zagreb, Croatia

<sup>3</sup>Faculty of Mechanical Engineering and Naval Architecture, University of Zagreb,  
Ivana Lučića 5, 10000 Zagreb, Croatia

(Received March 3, 2017, Revised April 13, 2017, Accepted April 20, 2017)

**Abstract.** Bora is a strong, usually dry temporally and spatially transient wind that is common at the eastern Adriatic Coast and many other dynamically similar regions around the world. One of the Bora main characteristics is its gustiness, when wind velocities can reach up to five times the mean velocity. Bora often creates significant problems to traffic, structures and human life in general. In this study, Bora velocity and near-ground turbulence are studied using the results of three-level high-frequency Bora field measurements carried out on a meteorological tower near the city of Split, Croatia. These measurements are analyzed for a period from April 2010 until June 2011. This rather long period allows for making quite robust and reliable conclusions. The focus is on mean Bora velocity, turbulence intensity, Reynolds shear stress and turbulence length scale profiles, as well as on Bora velocity power spectra and thermal stratification. The results are compared with commonly used empirical laws and recommendations provided in the ESDU 85020 wind engineering standard to question its applicability to Bora. The obtained results report some interesting findings. In particular, the empirical power- and logarithmic laws proved to fit mean Bora velocity profiles well. With decreasing Bora velocity there is an increase in the power-law exponent and aerodynamic surface roughness length, and simultaneously a decrease in friction velocity. This indicates an urban-like velocity profile for smaller wind velocities and a rural-like velocity profile for larger wind velocities. Bora proved to be near-neutral thermally stratified. Turbulence intensity and lateral component of turbulence length scales agree well with ESDU 85020 for this particular terrain type. Longitudinal and vertical turbulence length scales, Reynolds shear stress and velocity power spectra differ considerably from ESDU 85020. This may have significant implications on calculations of Bora wind loads on structures.

**Keywords:** Bora wind; gusts; velocity profile; thermal stratification; turbulence intensity; Reynolds shear stress; turbulence length scales; velocity power spectra; field measurements

### 1. Introduction

Bora is a vigorous, temporally and spatially transient, usually dry downslope wind. Its mean wind velocities rarely exceed 30 m/s, while one of Bora main characteristics is gustiness when the wind velocity may reach up to five times the mean velocity (e.g., Petkovšek 1987, Belušić and Klaić 2004, 2006, Grisogono and Belušić 2009, Večenaj *et al.* 2010, Belušić *et al.* 2013). It is more

---

\*Corresponding author, Associate Professor, E-mail: [hkozmar@fsb.hr](mailto:hkozmar@fsb.hr)

common in winter when it can last from just a few hours up to several days (e.g., Jurčec 1981, Poje 1992, Enger and Grisogono 1998, Kuzmić *et al.* 2015). It is more frequent at the eastern Adriatic and weakens seaward from the shore in a way that it is rarely stormy over the western Adriatic (e.g., Poje, 1992, Grisogono and Belušić 2009, Kuzmić *et al.* 2015). There is no unique and strict definition of Bora due to its extreme spatial variability, but a certain data set can be considered as a potential Bora event in case the horizontal velocity time series has the azimuth from the first quadrant and it is persistent for at least three hours with mean wind velocities larger or equal to 5 m/s and with standard deviation comparable to the mean value.

Bora significantly influences vehicles and structures (e.g., Kozmar *et al.* 2012a, b, 2014, 2015), especially in locations where it occurs rather frequently, like the town of Senj, Croatia, where Bora blows on average 177 days a year (e.g., Belušić and Klaić 2004). The Bora effects are to some extent comparable to wind effects of other transient winds, e.g., Solari (2014), Aboshosha and El Damatty (2015), Solari *et al.* (2015), Yang and Zhang (2016), Lou *et al.* (2016). Due to Bora, the ferry traffic among the coastal ports and the islands usually stops, airports remain closed to traffic for several days, as well as the major roads and freeways. Bora can cause vehicles to roll over or slide away from the road, blow off roofs and building facades. It can damage cable-supported bridges as well. For example, the Dubrovnik cable-supported bridge is considerably damaged in several severe Bora episodes in 2005 and 2006. Wind energy structures cannot operate during strong Bora events because they experience structural loading considerably larger than wind turbines in areas without Bora (e.g., Kozmar *et al.* 2016). Bora blows down the trees, causing larger areas or even entire counties to be without electricity due to collapsing electricity poles. There are not many records of building collapses due to Bora, because the buildings in coastal Croatia are generally low-rise and made of concrete that makes them not very prone to wind effects. However, in other dynamically similar places it is likely that Bora gusts will impact engineering structures. The wildfires are significantly enhanced when the Bora blows, similarly as for Santa Ana winds in Southern California (e.g., Cao and Fovell 2016).

Long lasting Bora occurrence is usually related to the presence of persistent cyclones over the Adriatic region and/or high pressure center over the Central Europe when the cyclone draws continental air from the lower troposphere across the mountain ranges (e.g., Jurčec 1981, Smith 1987, Heimann 2001, Belušić *et al.* 2013). Similarly, the air from the Pannonia Basin and the Central Europe is forced across coastal mountains toward the Adriatic by the anticyclone. Shallow or deep Bora occurs depending on the intensity and evolution of the cyclogenesis and its synchronization with the flow from the upper troposphere (e.g., Grisogono and Belušić 2009, Kuzmić *et al.* 2015). A passage of the cold front across the Adriatic can trigger a short lasting Bora. Depending on the triggering system, Bora can be cyclonic, anticyclonic or frontal. Cyclonic Bora occurs in the cold sector of the cyclone, when a deep cyclone engulfs at least a part of the Mediterranean. It is accompanied by a cloudy and windy weather, often with clouds and high possibility for precipitation. Anticyclonic (clear) Bora blows under the dominant influence of a high pressure field over most of Europe. It is relatively long-lasting accompanied by clear weather. Frontal Bora is associated with the passage of cold air behind a cold front. Its main characteristics are rapid onset and short duration (e.g., Jurčec and Visković 1994, Pandžić 2002).

The progress in basic understanding of the triggering system for the severe Bora developed along with development of advanced measurement systems and numerical atmospheric models. A problem with the katabatic-type perspective was that simple katabatic flows are unable to create continuous wind velocities of around 20 m/s. At the moment, a hydraulic theory of strong to severe Bora with orographic wave breaking is commonly adopted in the mesoscale community (Smith

1987, Klemp and Durran 1987, Enger and Grisogono 1998, Grubišić 2004, Grisogono and Belušić 2009). Strong Bora flow can to a good approximation be treated as a nonlinear hydraulic flow with a lack of significant stratification effects in the area of largest wind speeds (Klemp and Durran 1987, Smith 1987). That means that the resonance between the flow and underlying terrain is so strong that the wave breaking (thus mechanically-induced turbulence) dominates over thermal stratification effects (related to e.g., thermally-induced turbulence) near the ground (e.g., Lepri *et al.* 2014). Bora gusts usually exhibit quasi-periodic behavior (Petkovšek 1976, 1982, 1987, Rakovec 1987, Neiman *et al.* 1988). Bora pulsations usually occur at frequencies between 3 and 11 minutes (Belušić *et al.* 2004, 2006, 2007).

While Bora is characteristic for the eastern Adriatic Coast, it is recorded in other dynamically similar places around the world as well (e.g., Grisogono and Belušić 2009), thus making Bora research globally applicable. For example, downslope winds with similar dynamics are reported to occur in Austria, Iceland, Japan, Russia, USA, etc. (e.g., Jurčec 1981, Neiman *et al.* 1988, À gústsson and Ólafsson 2007, Jackson *et al.* 2013).

In this study, three level high-frequency measurements carried out on the meteorological tower close to Split, Croatia, are reported. The shape of characteristic Bora profiles, near-ground turbulence, velocity power spectra and thermal stratification are analyzed for the period of fourteen months. This rather long period guarantees a robustness and universality of the results. The results are compared with commonly used empirical laws and recommendations provided in the ESDU 85020 (1985) wind engineering standard to question its applicability on Bora wind.

## 2. Methodology

Field measurements are carried out from April 2010 until June 2011 at the meteorological tower Pometeno brdo (exact geographical coordinates 43°36'28.9"N and 16°28'37.4"E, 618 m above the mean sea level), Fig. 1. This location is in the hinterland of Split, Croatia on the lee side of the central Dinaric Alps, whereas the vegetation surrounding the measurement site is mostly shrubs and bushes lower than 3 m. The area is known for strong and frequent Bora occurrences (e.g., Makjanić 1978, Jurčec 1981).

Northern, eastern and vertical wind velocity components, as well as the ultrasonic temperature, are measured using Windmaster Pro (Gill instruments) ultrasonic anemometers at the sampling frequency of 5 Hz. Anemometers are mounted on a 60 m high meteorological tower at 10, 22 and 40 m facing the main Bora direction. The data is collected using the solar-powered Campbell Scientific data logger CR1000.

Before analyzing the data, it is necessary to control the data quality (e.g., Pandžić 2002) and remove the outliers. In order to prepare the data sets for further analysis, the very small amount of removed data is linearly interpolated. After the quality control is performed, the criteria for Bora is established, i.e., a) the NE wind direction with negative longitudinal and lateral velocity components, b) the wind blowing consistently for at least 10 h.

During the measurement period there are altogether 269 Bora episodes lasting from just a few hours up to 127 h. 119 Bora episodes lasting longer than 10 h are extracted and analyzed. In Table 1, the basic statistics for selected Bora episodes is chronologically represented with various Bora episodes referred to using their ordinal number (first column denoted with #). As expected, the wintertime Bora episodes generally last longer and have larger mean and maximum wind velocities than the summertime episodes, in agreement with Enger and Grisogono (1998). The #75

Bora episode, in total duration of 127 h, is overall the longest lasting Bora episode, the #63 has the largest maximal velocity and the #93 has the largest mean velocity. These three Bora episodes all occurred in wintertime. To study the seasonal variation of Bora turbulence characteristics, three summertime Bora episodes are selected for the analysis as well. In particular, the #12, in duration of 66 h, is the longest lasting summertime Bora episode, the #24 has the largest maximal velocity and the #16 has the largest mean velocity.

Time-averaged velocity is calculated using moving average of 17 min because previous work proved that  $17 \pm 3$  min represents a suitable turbulence averaging scale for Bora, i.e., a scale that separates turbulence at small scales from the mean flows at large scales (Magjarević *et al.* 2011). Hence, 17-min averaging period is considered to encompass all turbulence scales of interest for this study. Moreover, this is very close to 15 min as recently provided by Babić *et al.* (2016).

In the past, the power-law (Hellman 1916) proved to represent well the mean velocity profile throughout the entire atmospheric boundary layer (ABL), while the logarithmic law (Thuillier and Lappe 1964) is considered to be valid within the surface layer (roughly, the lowest 10-15% of the ABL). The applicability of the power-law on the Bora velocity profile is studied by calculating the power-law exponent,  $\alpha$ , and fitting the power-law to the profile made of measured mean velocities on all three heights. In particular, the time-averaged mean velocities in the  $x$ -direction at three levels are normalized using the time-averaged mean velocity in the  $x$ -direction at 40 m height and fitted to the power-law. To test the logarithmic-law, friction velocity,  $u_*$ , and aerodynamic surface roughness length,  $z_0$ , are calculated in two different ways, i.e., by data adjustment to the logarithmic-law, and by directly applying the logarithmic-law to a layer between 10 and 40 m (Lepri *et al.* 2014).

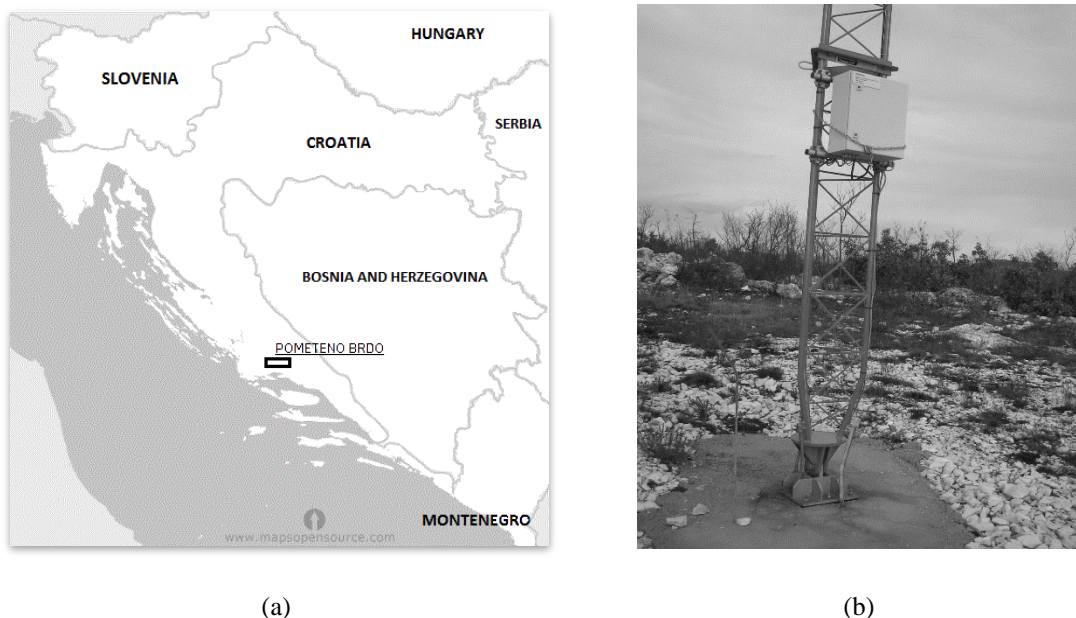


Fig. 1 (a) The geographical position of Pommeteno brdo (Swiped-Away Hill;  $43^{\circ}36'28.9''\text{N}$  and  $16^{\circ}28'37.4''\text{E}$ , 618 m above the mean sea level) on the geographical map of Croatia and (b) The pedestal of the meteorological tower. The vegetation around the measurement site consists mostly of low shrubs and bushes

Table 1 Basic statistics for analyzed Bora episodes

#	Start	End	Total duration (h)	$V_{av10}$ (m/s)	$V_{av22}$ (m/s)	$V_{av40}$ (m/s)	$V_{max10}$ (m/s)	$V_{max22}$ (m/s)	$V_{max40}$ (m/s)
1	16.04.2010	17.04.2010	17	6.5	7.3	7.5	15.3	15.4	15.6
2	17.04.2010	18.04.2010	11	5.4	5.8	6.2	10.5	10.3	10.3
3	28.04.2010	29.04.2010	14	7.5	8.5	9.1	18.2	18.4	18.9
4	18.05.2010	19.05.2010	13	5.0	6.0	6.4	13.6	13.2	13.2
5	19.05.2010	21.05.2010	33	7.6	9.2	9.9	20.1	21.8	22.2
6	21.05.2010	21.05.2010	16	7.1	8.5	9.4	16.6	18.5	17.7
7	22.05.2010	23.05.2010	15	5.5	6.8	7.8	17.1	18.0	18.2
8	23.05.2010	23.05.2010	11	4.1	4.7	4.9	11.4	11.9	11.4
9	23.05.2010	24.05.2010	13	4.6	5.1	5.2	11.1	12.7	10.2
10	04.06.2010	05.06.2010	23	6.3	7.6	8.2	18.0	19.2	20.0
11	05.06.2010	06.06.2010	11	4.6	5.1	5.3	10.3	10.2	10.3
12	22.06.2010	25.06.2010	66	7.2	8.6	9.2	24.8	25.6	23.8
13	27.06.2010	28.06.2010	15	5.5	6.7	7.5	16.9	16.8	18.3
14	18.07.2010	19.07.2010	17	6.0	6.8	6.8	17.6	16.6	16.7
15	19.07.2010	20.07.2010	14	4.2	4.6	4.8	9.8	11.0	9.9
16	24.07.2010	27.07.2010	62	9.0	10.6	11.4	24.9	24.9	25.7
17	31.07.2010	01.08.2010	10	3.5	3.8	4.1	10.8	10.7	10.6
18	08.08.2010	08.08.2010	11	3.6	4.0	4.2	10.2	10.5	10.0
19	08.08.2010	09.08.2010	10	2.2	2.6	2.9	4.8	5.2	5.2
20	09.08.2010	10.08.2010	11	3.1	3.4	3.6	6.1	6.5	6.3
21	10.08.2010	11.08.2010	12	3.3	3.7	3.9	9.7	10.0	10.1
22	11.08.2010	12.08.2010	10	2.5	2.9	3.2	5.1	5.2	5.4
23	21.08.2010	22.08.2010	20	5.0	5.7	6.0	13.0	13.5	16.4
24	28.08.2010	30.08.2010	34	7.6	8.9	9.5	27.2	29.4	28.9
25	30.08.2010	31.08.2010	10	4.7	5.7	6.6	10.5	11.5	12.0
26	01.09.2010	02.09.2010	11	3.9	4.4	4.5	10.7	10.5	11.0
27	05.09.2010	06.09.2010	10	3.5	3.8	4.0	7.3	7.5	7.8

Continued-

28	10.09.2010	12.09.2010	48	8.1	9.5	10.1	22.5	22.8	23.4
29	12.09.2010	13.09.2010	15	3.4	3.9	4.1	8.4	10.2	9.4
30	13.09.2010	15.09.2010	36	5.0	5.8	6.2	15.1	16.3	15.5
31	19.09.2010	21.09.2010	36	5.6	6.6	7.0	17.6	18.1	18.5
32	21.09.2010	22.09.2010	14	4.5	5.0	5.1	10.5	10.6	9.9
33	22.09.2010	23.09.2010	13	3.3	3.8	4.3	6.7	7.6	7.0
34	29.09.2010	30.09.2010	19	4.3	4.9	5.1	11.8	13.6	13.9
35	06.10.2010	09.10.2010	72	5.6	6.3	6.6	15.7	16.6	17.3
36	09.10.2010	10.10.2010	16	3.5	3.9	4.0	11.2	11.0	11.4
37	10.10.2010	11.10.2010	12	5.0	5.4	5.9	10.5	10.6	10.8
38	12.10.2010	13.10.2010	10	3.4	3.9	4.3	8.5	8.0	8.2
39	13.10.2010	15.10.2010	43	5.1	5.7	5.8	15.1	15.7	14.3
40	15.10.2010	16.10.2010	14	4.0	4.3	4.5	10.0	10.1	10.5
41	17.10.2010	20.10.2010	54	7.8	9.1	9.3	27.3	26.8	26.2
42	20.10.2010	21.10.2010	17	3.8	4.3	4.4	12.5	12.6	12.5
43	21.10.2010	22.10.2010	14	3.6	4.1	4.5	10.5	9.5	9.0
44	25.10.2010	28.10.2010	78	9.5	10.8	11.2	30.5	31.5	30.8
45	03.11.2010	04.11.2010	12	3.7	4.1	4.5	8.4	8.2	8.6
46	20.11.2010	20.11.2010	10	4.2	4.5	4.7	10.0	10.7	10.3
47	24.11.2010	25.11.2010	31	4.7	5.0	5.2	12.1	12.9	12.5
48	27.11.2010	28.11.2010	18	7.0	7.6	7.9	21.9	19.8	19.4
49	30.11.2010	30.11.2010	16	6.4	6.7	6.9	20.3	15.5	15.0
50	03.12.2010	04.12.2010	13	3.5	3.8	4.1	7.2	8.1	8.2
51	04.12.2010	04.12.2010	10	4.9	5.4	5.4	12.3	12.4	12.3
52	04.12.2010	05.12.2010	11	3.0	3.5	3.7	9.1	9.4	10.1
53	09.12.2010	10.12.2010	15	11.6	13.2	14.4	32.6	31.9	33.8
54	12.12.2010	17.12.2010	113	8.6	9.5	10.2	31.0	29.3	27.8
55	18.12.2010	19.12.2010	14	3.5	3.9	4.3	9.9	10.6	11.6
56	20.12.2010	21.12.2010	13	2.3	2.6	3.0	6.6	6.9	7.6
57	25.12.2010	28.12.2010	65	6.6	7.1	7.5	26.0	27.8	26.9
58	30.12.2010	31.12.2010	13	2.2	2.5	2.9	5.4	5.2	5.4

Continued-

59	02.01.2011	04.1.2011	44	8.0	8.5	9.2	30.1	27.2	27.3
60	04.01.2011	05.01.2011	11	3.4	3.7	4.1	7.8	8.6	8.2
61	11.01.2011	12.01.2011	11	2.6	2.8	3.1	6.1	6.7	6.8
62	12.01.2011	13.01.2011	14	3.7	4.2	4.5	10.3	11.2	11.3
63	20.01.2011	25.01.2011	117	11.2	11.8	12.1	40.9	36.7	35.2
64	26.01.2011	27.01.2011	16	6.9	7.3	7.5	16.2	13.8	13.7
65	27.01.2011	29.01.2011	45	8.5	8.7	9.0	17.8	16.3	15.9
66	29.01.2011	30.01.2011	13	4.7	5.0	5.2	9.8	9.8	9.6
67	31.01.2011	31.01.2011	13	5.3	5.6	5.8	11.6	12.7	10.9
68	01.02.2011	02.02.2011	13	2.5	2.9	3.3	6.4	7.0	7.1
69	02.02.2011	03.02.2011	28	10.2	11.2	11.6	23.5	24.0	23.9
70	03.02.2011	04.02.2011	27	8.5	9.7	10.3	26.3	26.9	25.9
71	06.02.2011	07.02.2011	13	2.1	2.5	2.9	5.4	6.0	6.7
72	09.02.2011	10.02.2011	15	3.8	4.2	4.5	11.0	11.2	11.1
73	17.02.2011	18.02.2011	15	5.2	5.5	5.8	12.9	13.3	12.9
74	18.02.2011	20.02.2011	43	8.2	9.1	9.8	20.8	21.5	20.7
75	21.02.2011	26.02.2011	127	11.4	12.6	13.1	31.9	33.0	32.0
76	28.02.2011	01.03.2011	13	7.5	8.2	8.6	15.0	15.8	14.8
77	02.03.2011	03.03.2011	12	7.0	7.6	8.2	14.7	15.6	14.6
78	03.03.2011	04.03.2011	15	5.8	6.2	6.3	13.4	13.3	14.0
79	04.03.2011	05.03.2011	19	3.7	4.1	4.3	9.1	9.9	8.6
80	06.03.2011	08.03.2011	46	11.7	13.3	14.5	35.8	37.1	34.8
81	08.03.2011	09.03.2011	24	7.1	7.8	8.1	24.3	23.8	24.4
82	18.03.2011	22.03.2011	84	10.9	12.0	13.0	27.4	28.3	28.5
83	22.03.2011	23.03.2011	17	5.9	6.8	7.1	16.7	16.0	15.9
84	23.03.2011	23.03.2011	10	4.4	5.0	5.4	14.2	15.4	15.5
85	23.03.2011	24.03.2011	19	7.3	8.2	8.6	18.6	19.4	19.5
86	28.03.2011	29.03.2011	15	5.8	6.3	6.6	13.7	14.0	14.3
87	01.04.2011	02.04.2011	23	6.7	7.7	8.4	17.8	17.5	17.6
88	02.04.2011	03.04.2011	26	4.6	5.2	5.7	16.8	16.9	16.9
89	05.04.2011	06.04.2011	35	9.7	11.0	11.9	25.6	27.4	26.2

Continued-

90	06.04.2011	07.04.2011	18	7.6	9.0	10.0	23.4	26.4	24.9
91	09.04.2011	10.04.2011	22	7.4	8.6	9.3	23.3	25.3	25.0
92	11.04.2011	12.04.2011	14	6.1	7.1	7.3	16.6	18.6	15.6
93	13.04.2011	13.04.2011	18	12.3	14.2	15.0	30.6	28.6	34.6
94	15.04.2011	17.04.2011	58	7.9	8.9	9.4	19.9	20.6	19.9
95	17.04.2011	18.04.2011	25	7.6	8.7	9.2	18.4	18.9	18.5
96	18.04.2011	19.04.2011	14	5.2	5.7	5.8	12.4	13.0	13.0
97	19.04.2011	20.04.2011	14	4.7	5.7	6.2	12.0	13.5	13.1
98	27.04.2011	28.04.2011	19	3.5	3.9	4.1	13.3	14.2	13.8
99	30.04.2011	01.05.2011	17	6.2	7.0	7.3	15.6	15.6	15.1
100	03.05.2011	03.05.2011	17	7.0	7.8	8.0	18.6	17.7	17.4
101	03.05.2011	06.05.2011	59	7.6	8.9	9.7	24.3	23.7	23.6
102	08.05.2011	10.05.2011	52	11.5	13.4	13.8	32.3	33.4	32.8
103	11.05.2011	12.05.2011	15	6.4	7.8	7.7	21.5	22.5	23.6
104	13.05.2011	14.05.2011	13	3.3	3.7	3.9	9.3	9.5	10.8
105	16.05.2011	18.05.2011	55	9.9	11.7	12.6	28.2	29.1	28.4
106	18.05.2011	19.05.2011	12	4.5	5.2	5.7	12.3	12.6	12.9
107	21.05.2011	22.05.2011	20	4.3	4.9	5.2	15.2	15.7	16.8
108	23.05.2011	24.05.2011	19	4.3	5.1	5.5	11.8	13.3	13.7
109	24.05.2011	26.05.2011	39	7.3	8.6	8.7	20.1	19.6	19.2
110	29.05.2011	29.05.2011	11	4.6	5.2	5.4	13.0	13.6	13.4
111	29.05.2011	30.05.2011	19	5.2	6.1	6.4	13.8	14.1	15.0
112	01.06.2011	02.06.2011	15	2.8	3.2	3.5	9.7	9.9	9.9
113	02.06.2011	03.06.2011	20	6.6	7.7	8.0	16.5	16.8	16.6
114	03.06.2011	04.06.2011	12	4.5	5.0	5.2	10.4	10.2	11.1
115	10.06.2011	11.06.2011	13	4.3	5.0	5.2	12.2	13.1	13.4
116	11.06.2011	12.06.2011	17	6.3	7.4	8.2	15.1	16.0	16.5
117	12.06.2011	13.06.2011	17	4.3	4.9	5.2	11.3	11.5	12.4
118	13.06.2011	14.06.2011	13	3.7	4.1	4.2	8.0	8.4	8.8
119	14.06.2011	15.06.2011	16	4.9	5.5	5.7	14.6	15.4	15.4

---

Furthermore, the obtained values are compared with values reported in Table 2 (ESDU 85020 1985). Turbulence intensity is defined as the root-mean-square of the fluctuating velocity components normalized with the local time-averaged velocity (Simiu and Scanlan 1996). Reynolds shear stress is calculated using the fluctuating velocity correlations  $-\rho\overline{u'v'}$ ,  $-\rho\overline{v'w'}$ ,  $-\rho\overline{u'w'}$ , where  $\rho$  is air density. The length scales of turbulence in the  $x$ -direction related to  $u'$ ,  $v'$ ,  $w'$  fluctuations are calculated using autocorrelation functions and assuming the validity of the Taylor's frozen turbulence hypothesis (e.g. ESDU 74030 1976). The procedure for calculation of turbulence intensity, Reynolds shear stress and turbulence length scales is described in Lepri *et al.* (2015) for a single summertime Bora episode and now applied on all 119 analyzed Bora episodes. Prior to calculating Bora turbulence parameters, 17-min moving average is deduced from the velocity time history to remove the long-wave meandering from the time history, as this long-wave meandering is not considered as turbulence. The results obtained for turbulence intensity, Reynolds shear stress and turbulence length scales are compared with the values recommended in ESDU 85020 (1985).

The dimensionless stability parameter,  $\zeta$ , (e.g., Stull 1988) is used to describe thermal stratification. It is calculated using the expression

$$\zeta = \frac{z}{L} \quad (1)$$

Table 2 Typical values of terrain parameters  $z_0$  and  $d$  reported in ESDU 85020 (1985);  $\alpha$  is calculated as  $\alpha = 0.0961 (\log z_0) + 0.016 (\log z_0)^2 + 0.24$  (Counihan 1975)

Terrain description	$\alpha$ (-)	$z_0$ (m)	$d$ (m)
City centers Forests	0.23	0.7	15 to 25
Small towns Suburbs of large towns and cities Wooded country (many trees)	0.19	0.3	5 to 10
Outskirts of small towns Villages Countryside with many hedges, some trees and some buildings	0.16	0.1	0 to 2
Open level country with few trees and hedges and isolated buildings; typical farmland	0.13	0.03	0
Fairly level grass plains with isolated trees	0.11	0.01	0
Very rough sea in extreme storms (once in every 50 years extreme) Flat areas with short grass and no obstructions Runway area of airports	0.10	0.003	0
Rough sea in annual extreme storms Snow covered farmland Flat desert or arid areas Inland lakes in extreme storms	0.10	0.001	0

where  $L$  is Obukhov length and  $z$  is height above the ground. Positive  $\zeta$  implies statically stable, negative  $\zeta$  implies statically unstable and  $\zeta = 0$  implies statically neutral thermal stratification.

The frequency distribution of fluctuating wind velocity is particularly important when calculating dynamic wind effects on structures. Hence, power spectral density of Bora fluctuations is calculated for all three velocity components on all three height levels using the methodology described in Stull (1988) and compared with ESDU 85020 (1985).

### 3. Results and discussion

In this section, important aspects of mean Bora velocity, turbulence intensity, Reynolds shear stress, turbulence length scale profiles along with velocity power spectra and thermal stratification are analyzed.

The power-law exponent, one value of  $\alpha$  for each Bora episode, has values in the range up to 0.3 (Fig. 2(b)). Larger mean values of  $\alpha$  are accompanied with larger mean velocity at 40 m height. The observed behavior of vertical velocity profile indicates an urban-like velocity profile at smaller wind velocities and a rural-like velocity profile at larger wind velocities. In the agreement with results previously reported for a single summertime Bora episode (Lepri *et al.* 2014),  $z_0$  and  $u_*$  calculated using the logarithmic-law fit and by directly applying logarithmic law to a layer between 10 and 40 m are nearly the same (Figs. 2(c)-2(f)). Figs. 2(e) and 2(f) represent the median value of calculated  $z_0$  because Lepri *et al.* (2014) showed that due to Poisson-like distribution of  $z_0$ , the more robust median represents a more suitable parameter to describe  $z_0$  than its mean value. Friction velocity ranges between 0 and 1 m/s with mean values between 0.1 and 0.8 m/s (Figs. 2(c) and (d)). The median values of  $z_0$  are mostly in the range from 0.0 to 0.2 m with largest values around 0.6 m. The standard deviations of  $z_0$  are rather large, especially for episodes with larger median values of  $z_0$ .

Figs. 3-5 represent mean turbulence intensity in the  $x$ -,  $y$ - and  $z$ -direction on all three heights reported along with the mean wind velocity at 40 m height. The obtained values are compared with ESDU 85020 (1985) for  $z_0 = 0.03$  m. The values of all three turbulence intensity components decrease with height. The obtained mean values of  $I_u$  and  $I_v$  are mostly in the range from 0.1 to 0.2, while the values of  $I_w$  are smaller and scattered around 0.1. Rather small values of standard deviation for all three components indicate small spread of values around the mean on all three height levels (e.g., Papoulis 2002). When compared with the ESDU 85020 (1985) values, it can be observed that mean values of all three turbulence intensity components agree well with the standard values.

Reynolds shear stress on all three levels reported along with the mean wind velocity at 40 m height in comparison with ESDU 85020 (1985) for  $z_0 = 0.03$  m is presented in Fig. 6. The obtained values do not fit well the ESDU 85020 (1985) values, possibly due to complex terrain effects, which are yet to be investigated in detail. The calculated absolute values are mostly smaller than the standard values, while the agreement is better at lower levels.

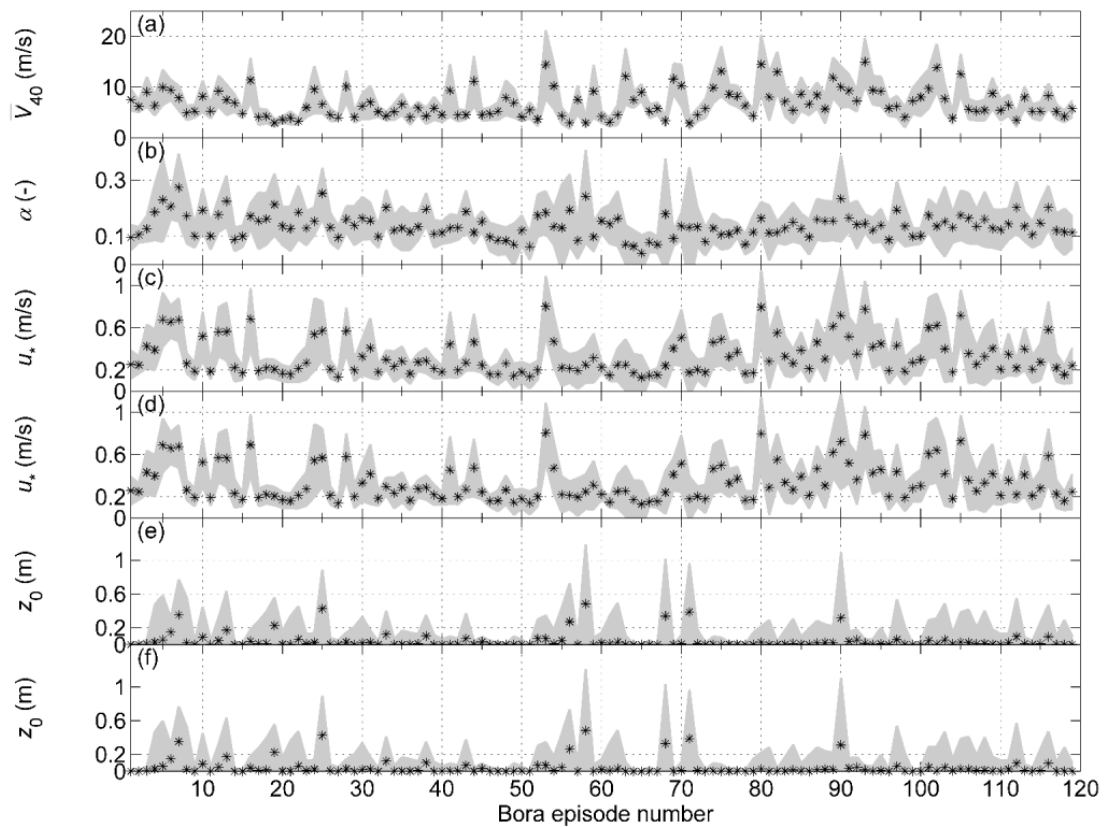


Fig. 2 (a) Mean wind velocity at 40 m, (b) mean power-law exponent, (c) mean friction velocity,  $u_*$ , obtained directly by applying the logarithmic law to a layer between 10 and 40 m, (d) mean friction velocity,  $u_*$ , calculated using the logarithmic-law adjustment, (e) median aerodynamic surface roughness length,  $z_0$ , calculated using logarithmic-law adjustment and (f) median aerodynamic surface roughness length,  $z_0$ , calculated using the logarithmic-law adjustment. The black star is mean/median value of particular parameter for each Bora episode. Gray shaded area represents standard deviation range for each Bora episode

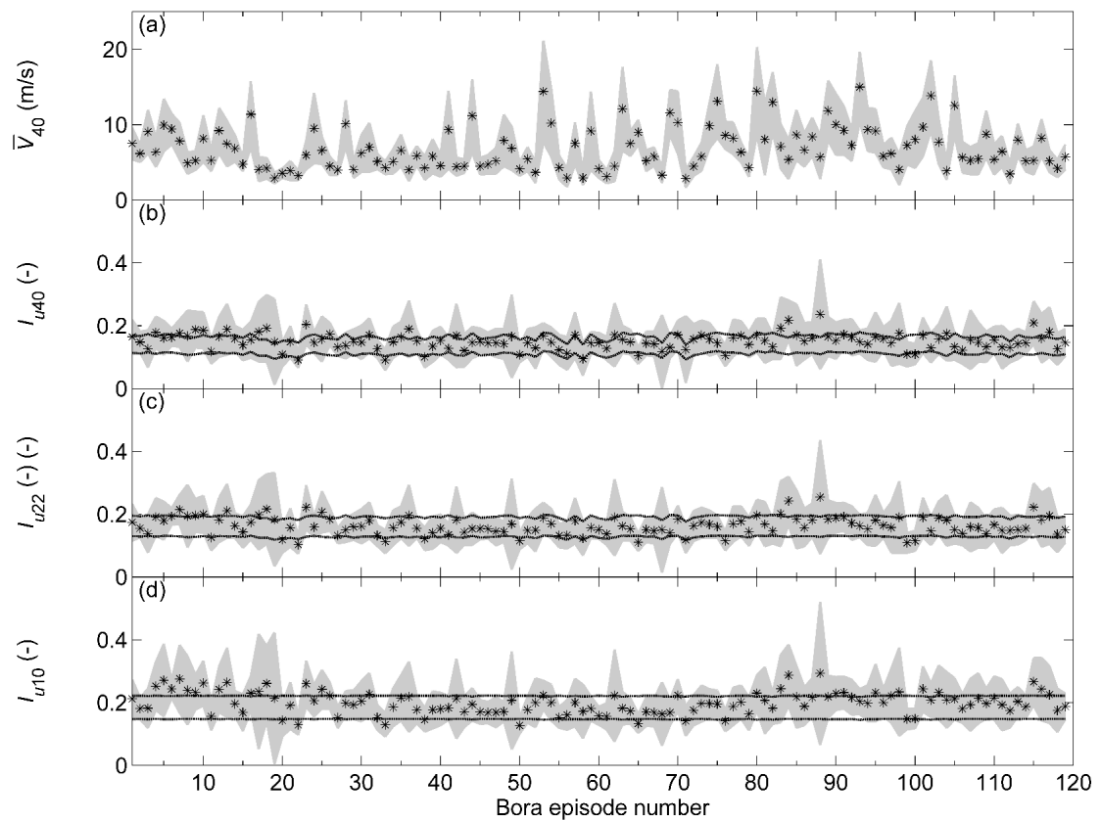


Fig. 3 (a) Mean wind velocity at 40 m; turbulence intensity in the  $x$ -direction at (b) 40 m height, (c) 22 m height and (d) 10 m height. The black star is mean value of turbulence intensity for each Bora episode. Gray shaded area represents standard deviation range of mean wind velocity and turbulence intensity for each Bora episode. Black dotted curve represents ESDU 85020 (1985) values for  $z_0 = 0.03$  m with tolerance range  $\pm 20\%$ . Standard values are separately calculated for each Bora episode

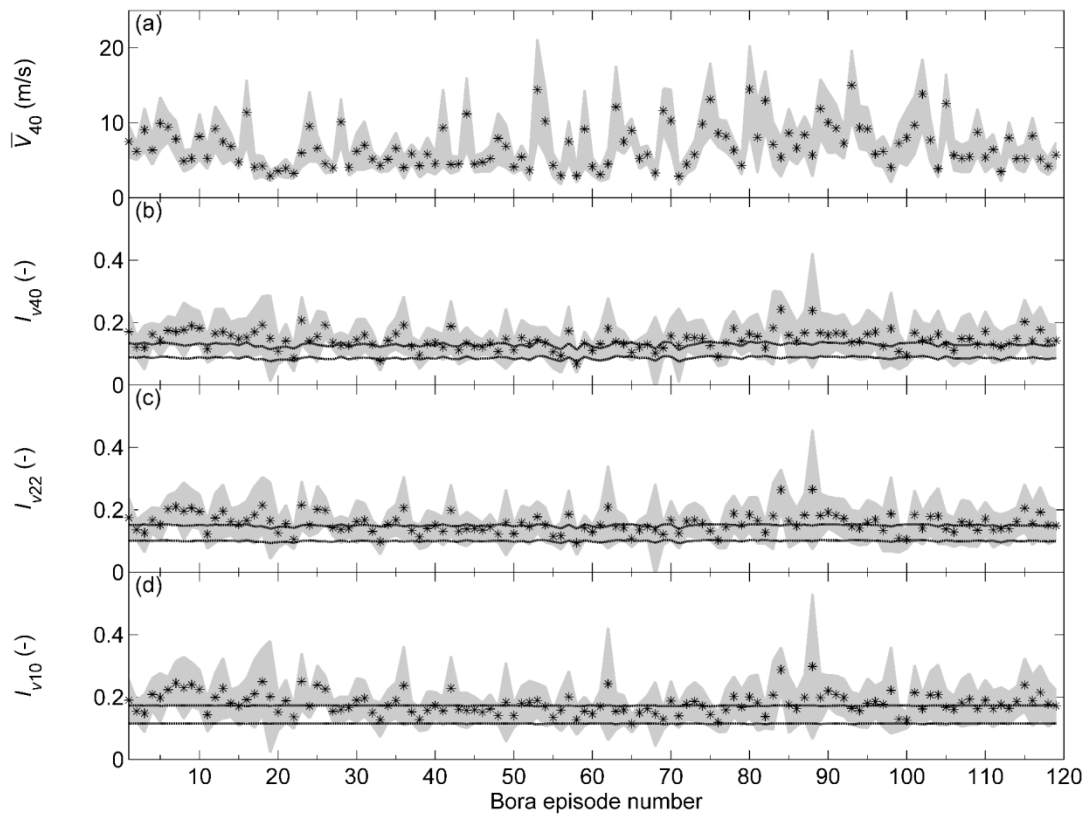


Fig. 4 (a) Mean wind velocity at 40 m; turbulence intensity in the  $y$ -direction at (b) 40 m, (c) 22 m and (d) 10 m height. The black star is mean value of turbulence intensity for each Bora episode. Gray shaded area represents standard deviation range of mean wind velocity and turbulence intensity for each Bora episode. Black dotted curve represents ESDU 85020 (1985) values for  $z_0 = 0.03$  m with tolerance range  $\pm 20\%$ . Standard values are separately calculated for each Bora episode

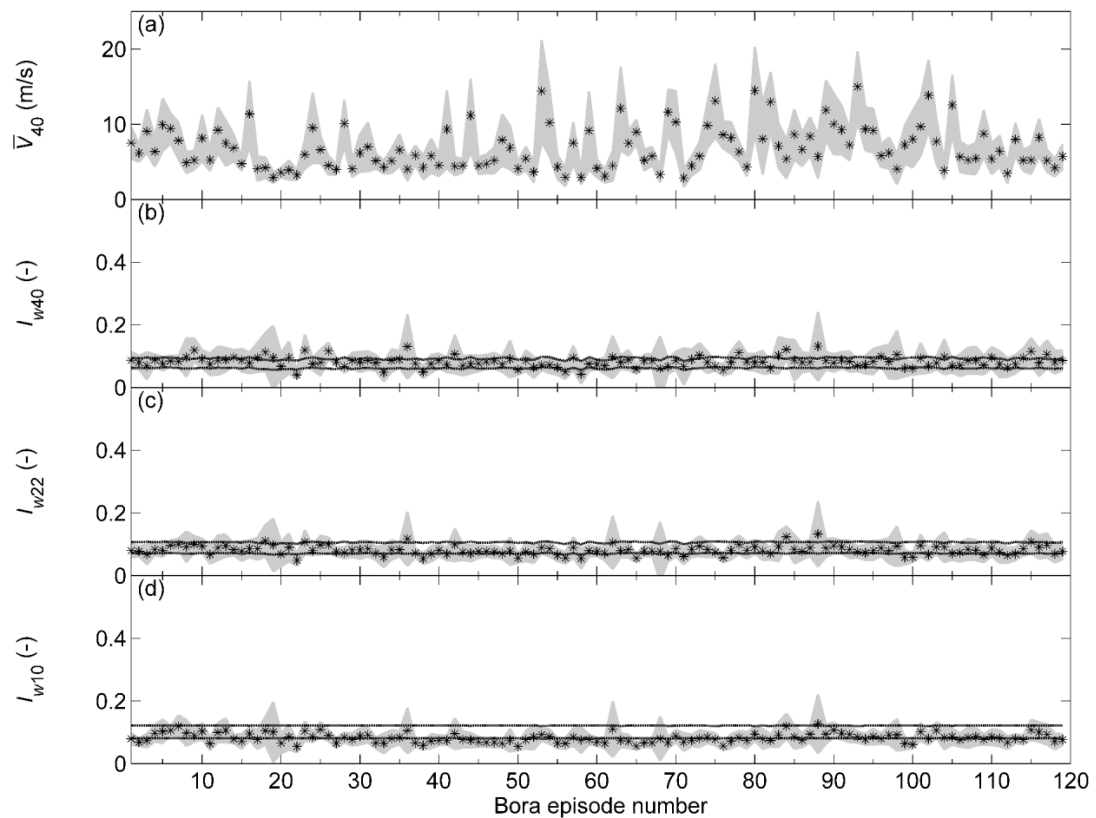


Fig. 5 (a) Mean wind velocity at 40 m; turbulence intensity in the  $z$ -direction at (b) 40 m, (c) 22 m and (d) 10 m height. The black star is mean value of turbulence intensity for each Bora episode. Gray shaded area represents standard deviation range of mean wind velocity and turbulence intensity for each Bora episode. Black dotted curve represents ESDU 85020 (1985) values for  $z_0 = 0.03$  m with tolerance range  $\pm 20\%$ . Standard values are separately calculated for each Bora episode

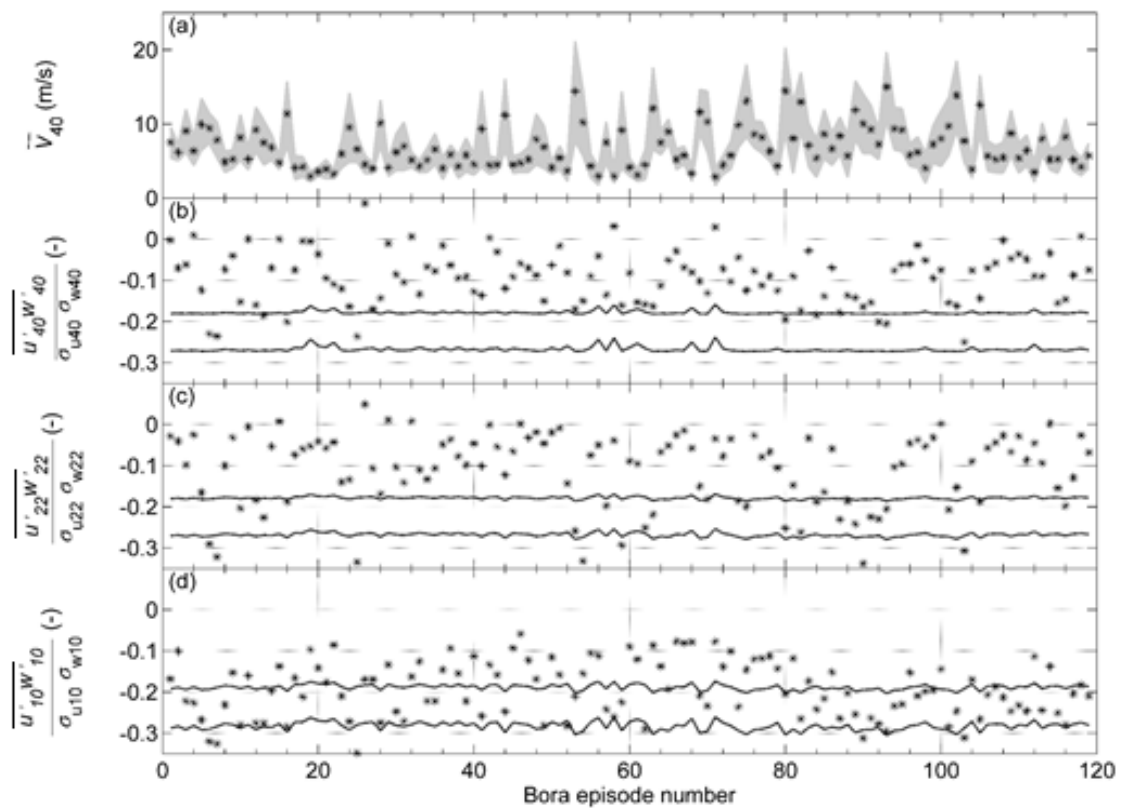


Fig. 6 (a) Mean wind velocity at 40 m; Reynolds shear stress at (b) 40 m, (c) 22 m and (d) 10 m height. The black star is mean value of observed  $\overline{u'w'}/\sigma_u\sigma_v$  for each Bora episode. Gray shaded area represents standard deviation range of mean wind velocity for each Bora episode. Black dotted curve represents ESDU 85020 (1985) values for  $z_0 = 0.03$  m with tolerance range  $\pm 20\%$ . Standard values are separately calculated for each Bora episode

Figs. 7-9 represent length scales of turbulence in the  $x$ -direction related to fluctuations  $u'$ ,  $v'$  and  $w'$  reported along with the mean wind velocity at 40 m height in comparison with ESDU 85020 (1985) data for  $z_0 = 0.03$  m.

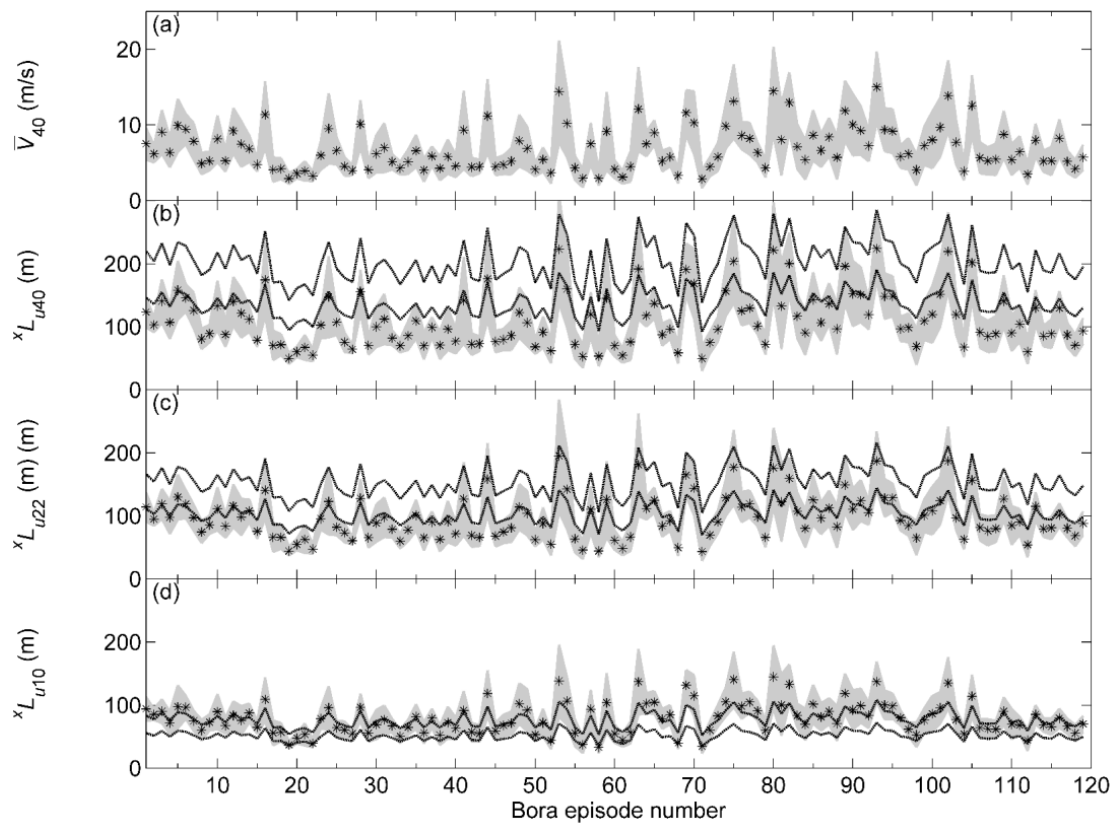


Fig. 7 (a) Mean wind velocity at 40 m; length scales of turbulence in the  $x$ -direction related to  $u'$  at (b) 40 m; (c) 22 m and (d) 10 m height. The black star is mean value of  ${}^xL_u$  for each Bora episode. Gray shaded area represents standard deviation range of mean wind velocity and  ${}^xL_u$  for each Bora episode. Black dotted curve represents ESDU 85020 (1985) values for  $z_0 = 0.03$  m with tolerance range  $\pm 20\%$ . Standard values are separately calculated for each Bora episode

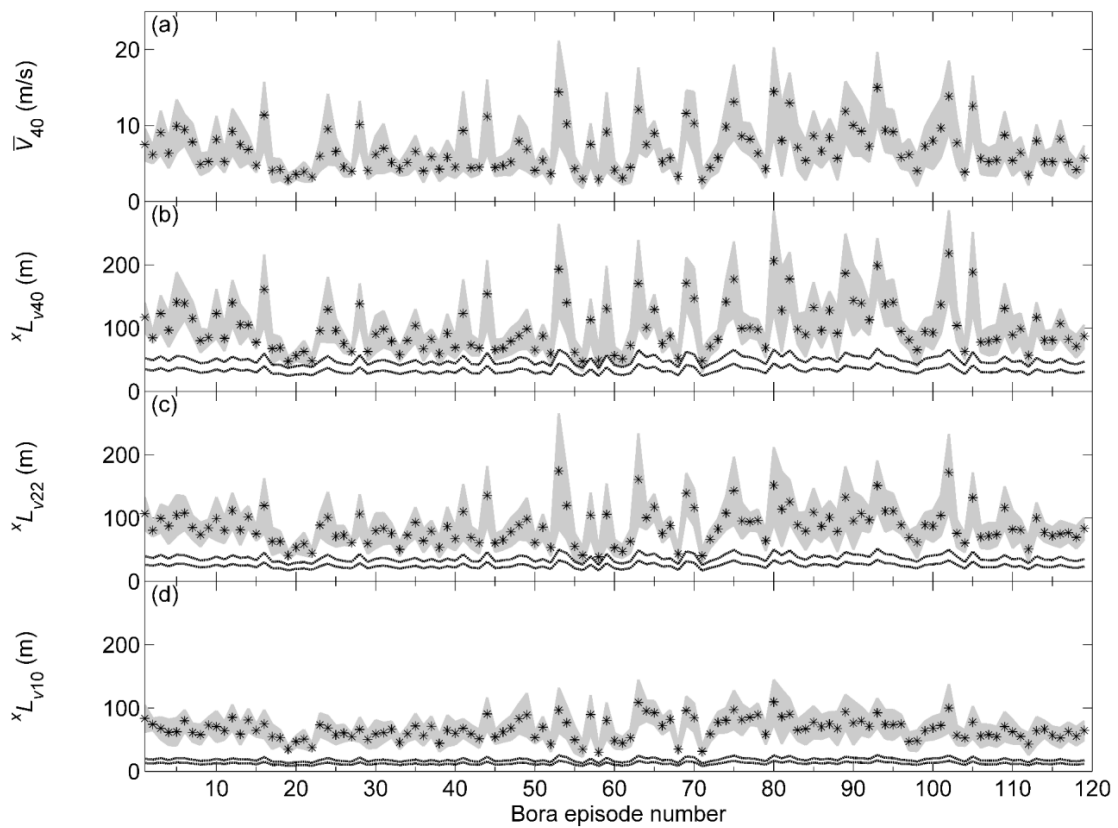


Fig. 8 (a) Mean wind velocity at 40 m; length scales of turbulence in the  $x$ -direction related to  $v'$  at (b) 40 m; (c) 22 m and (d) 10 m height. The black star is mean value of  ${}^xL_v$  for each Bora episode. Gray shaded area represents standard deviation range of mean wind velocity and  ${}^xL_v$  for each Bora episode. Black dotted curve represents ESDU 85020 (1985) values for  $z_0 = 0.03$  m with tolerance range  $\pm 20\%$ . Standard values are separately calculated for each Bora episode

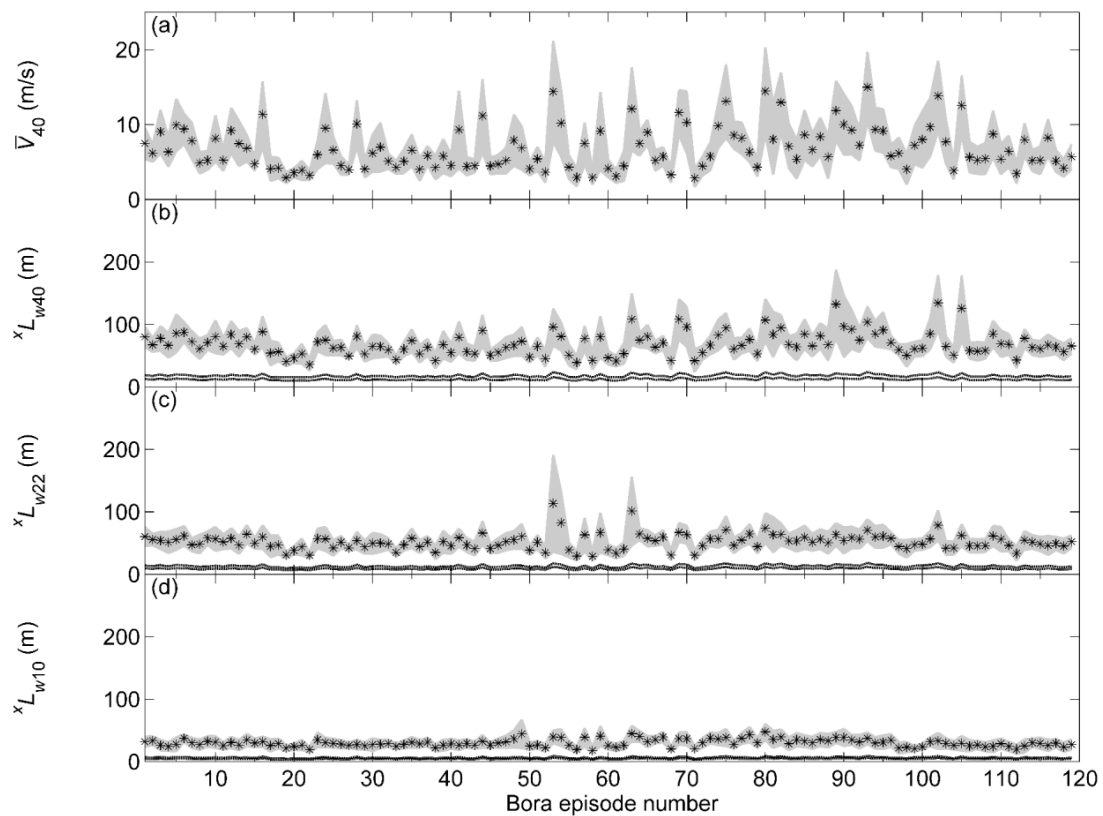


Fig. 9 (a) Mean wind velocity at 40 m; length scales of turbulence in the  $x$ -direction related to  $w'$  at (b) 40 m; (c) 22 m and (d) 10 m height. The black star is mean value of  ${}^xL_w$  for each Bora episode. Gray shaded area represents standard deviation range of mean wind velocity and  ${}^xL_w$  for each Bora episode. Black dotted curve represents ESDU 85020 (1985) values for  $z_0 = 0.03$  m with tolerance range  $\pm 20\%$ . Standard values are separately calculated for each Bora episode

All three components of turbulence length scales increase with height, which is in agreement with atmospheric physics (e.g., Stull 1988). The mean values of  $^xL_u$  range between 50 m at 10 m and 100 m at 40 m height. These values are generally in agreement with the ESDU 85020 (1985) values. The agreement is better at lower height levels, while for higher levels the obtained data are smaller than the standard values. The mean values of  $^xL_v$  range between 50 m at 10 m and 100 m at 40 m height. These values are significantly larger than the values proposed in ESDU 85020 (1985) on all three height levels. The mean values of  $^xL_w$  range between 25 m at 10 m height and 80 m at 40 m height. The obtained mean values are considerably larger than the standard values, most probably because of the plausible terrain induced ABL flow reattachment, recirculation and separation phenomena that will be further studied in the future.

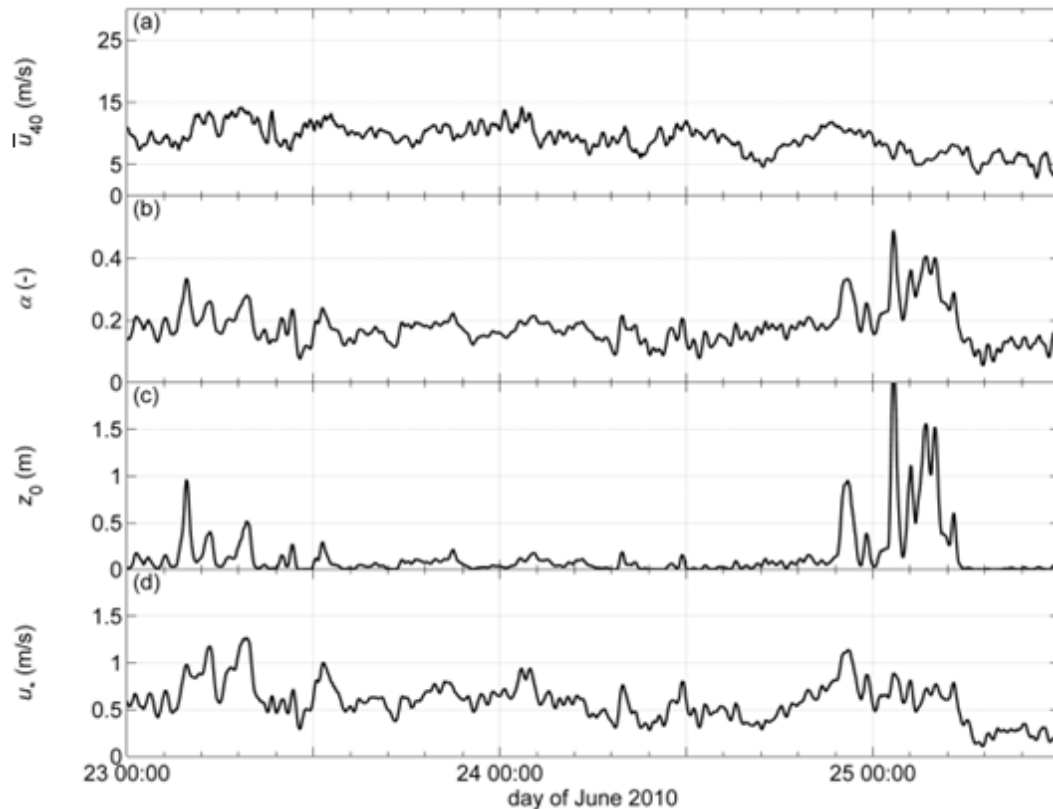


Fig. 10 Time series of (a) mean wind velocity in the main ( $x$ ) wind direction averaged over the time scale of 17 min at 40 m height, (b) power-law exponent  $\alpha$ , (c) friction velocity  $u_*$  calculated using the logarithmic adjustment and (d) aerodynamic surface roughness length  $z_0$  calculated using logarithmic adjustment for the #12 summertime Bora episode

Time series of the power law-exponent, friction velocity and surface roughness length as well as their seasonal variations are investigated next. To investigate seasonal variations of these parameters, one summertime Bora episode, the #12 episode, and one wintertime episode, the #75 episode, are selected to be representative for each season. Although commonly presented as a constant, the power-law exponent takes on a variety of values, suggesting a rural-like velocity profile for larger wind velocities and urban-like profile for smaller velocities (Figs. 10 and 11).

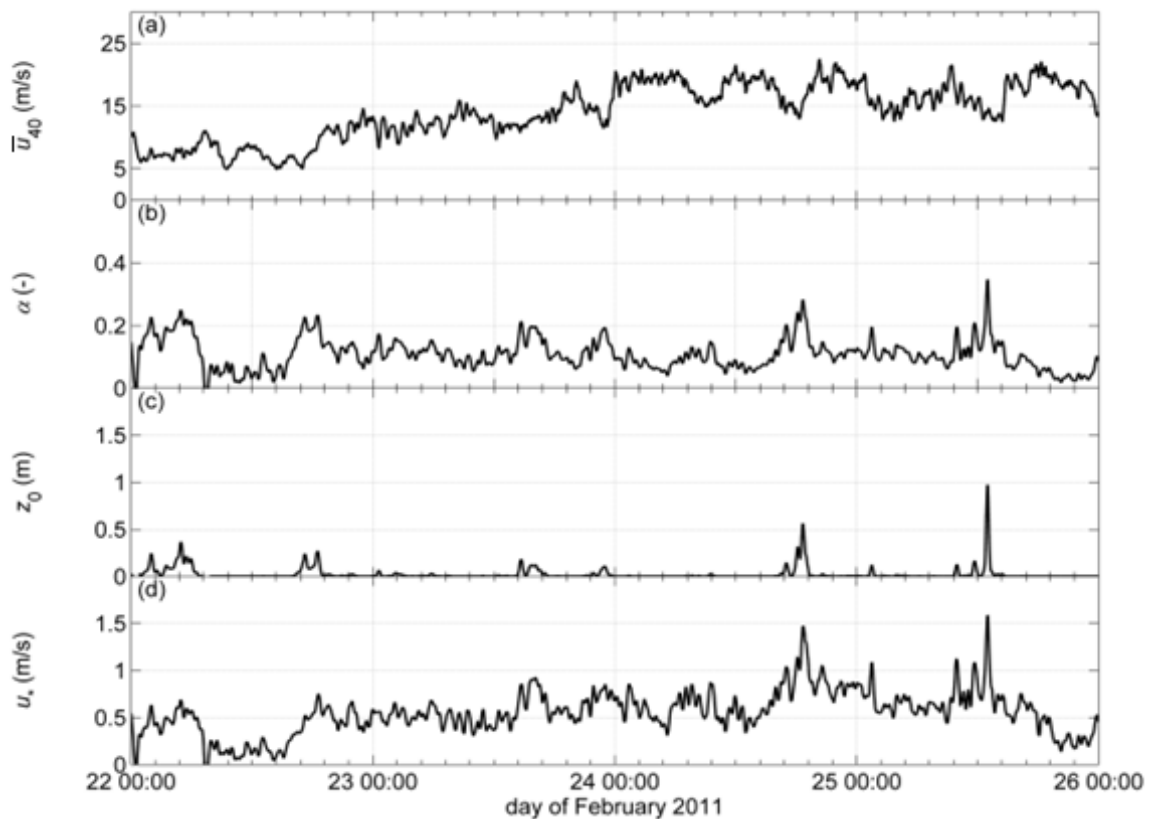


Fig. 11 Time series of (a) mean wind velocity in the main ( $x$ ) wind direction averaged over the time scale of 17 min at 40 m height, (b) power-law exponent  $\alpha$ , (c) friction velocity  $u_*$  calculated using the logarithmic adjustment and (d) aerodynamic surface roughness length  $z_0$  calculated using logarithmic adjustment for the #75 wintertime Bora episode

Furthermore, the values of friction velocity and aerodynamic surface roughness length vary considerably. The values of friction velocity and aerodynamic surface roughness length obtained by directly applying the logarithmic law to a layer between 10 and 40 m are not shown because they are nearly the same as the values obtained by logarithmic adjustment. Wintertime Bora episode is much stronger with larger wind velocities than the summertime episode. The power-law exponent, friction velocity and surface roughness length values have larger amplitudes and are more variable in summertime than in wintertime. Furthermore, the results show that both the logarithmic-law and the power-law fit the Bora wind velocity profiles rather well, both in summertime and in wintertime (Fig. 12).

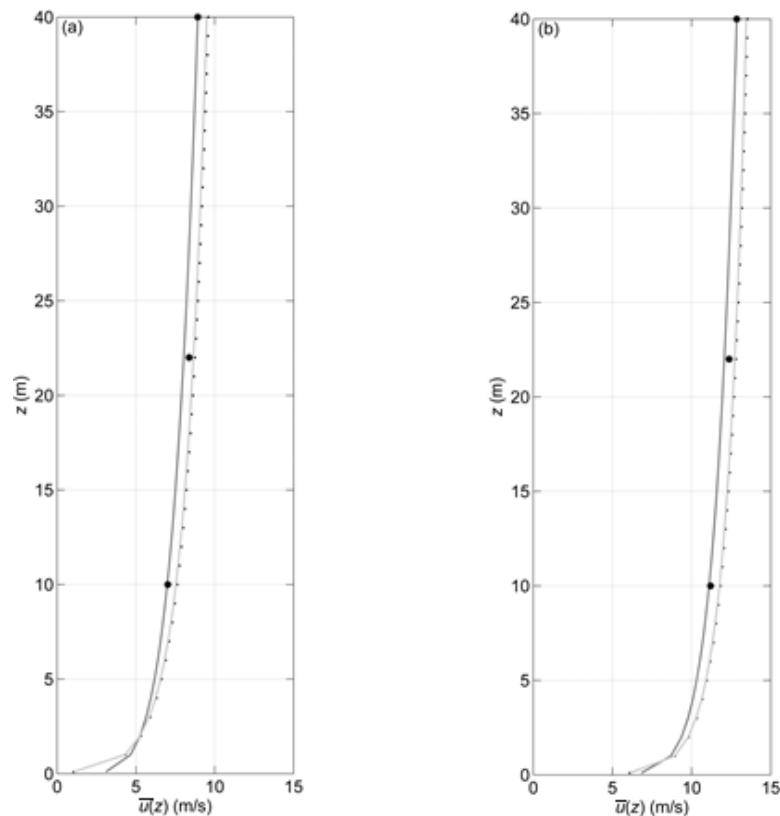


Fig. 12 Vertical velocity profile of the Bora wind; comparison with the logarithmic- and power-law; comparison based on calculation using the arithmetic mean value. Legend: star is measured arithmetic mean value during the Bora episode, black solid line is power-law, black dotted line is logarithmic-law, grey line is direct application of the logarithmic law to a layer between 10 and 40 m. (a) the #12 summertime Bora episode and (b) the #75 wintertime Bora episode

Figs. 13 and 14 represent time series for all three turbulence intensity components at three height levels along with the mean wind velocity. The largest values of all three turbulence intensity components are obtained at the lowest measurement level, 10 m, in agreement with atmospheric physics. Another interesting feature is the fact that for mean wind velocities larger than 5 m/s, turbulence intensity is almost constant while for smaller velocities it starts to fluctuate significantly.

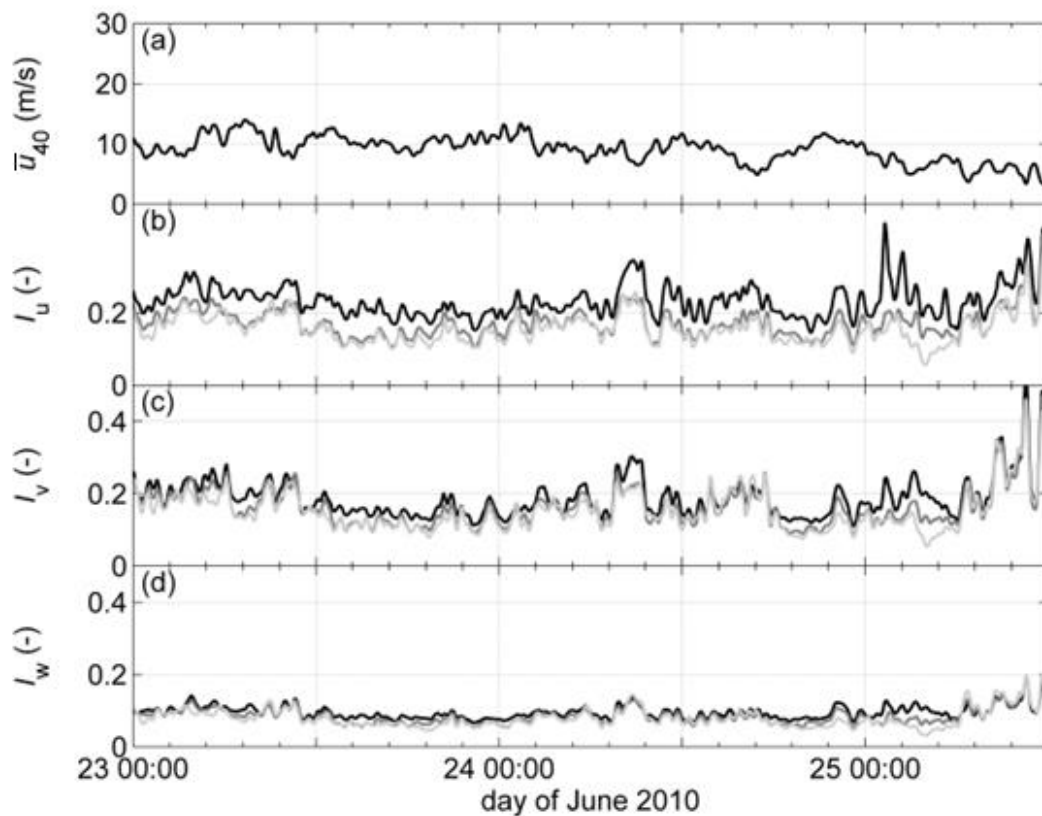


Fig. 13 Time series of (a) mean wind velocity in the main ( $x$ ) wind direction at 40 m height, (b) turbulence intensity in the  $x$ -direction, (c) turbulence intensity in the  $y$ -direction and (d) turbulence intensity in the  $z$ -direction. Black curve is turbulence intensity at 10 m, dark gray curve is turbulence intensity at 22 m and light gray is turbulence intensity at 40 m height for the #12 summertime Bora episode

The #12 summertime episode and the #63 wintertime episode are selected to analyze seasonal variability of turbulence intensity. Mean wind velocities, as well as maximal velocities in wintertime are much larger than in summertime. During periods of larger mean wind velocities in wintertime, all three components of turbulence intensity on all three levels are almost constant and start fluctuating when mean wind velocities drop below 5 m/s. On the other hand, summertime wind velocities are smaller and the values of turbulence intensity are larger than in wintertime with more pronounced fluctuations from mean wind velocities below 5 m/s. No day to night trends can be observed in both seasons.

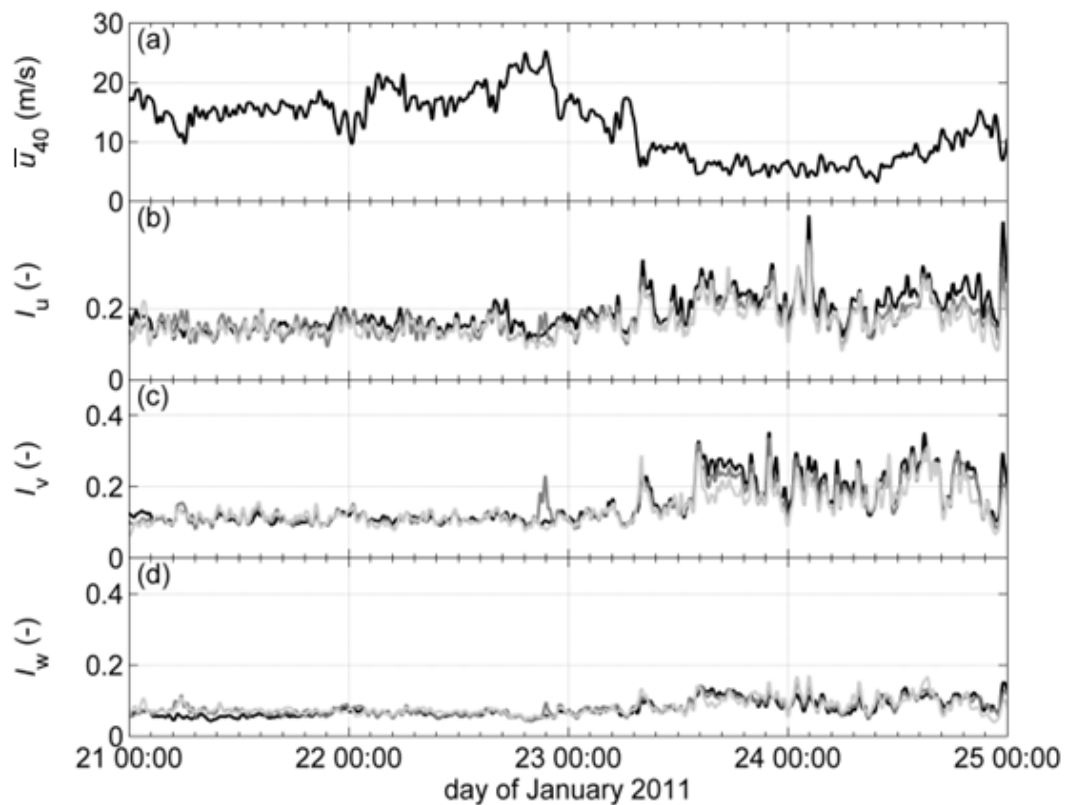


Fig. 14 Time series of (a) mean wind velocity in the main ( $x$ ) wind direction at 40 m height, (b) turbulence intensity in the  $x$ -direction, (c) turbulence intensity in the  $y$ -direction and (d) turbulence intensity in the  $z$ -direction. Black curve is turbulence intensity at 10 m, dark gray curve is turbulence intensity at 22 m and light gray is turbulence intensity at 40 m height for the #63 wintertime Bora episode

Figs. 15 and 16 show time series of three Reynolds shear stress components for each of the three measurement heights. The #63 wintertime Bora episode and the #12 summertime episode are selected for the analysis. The strongest component is the  $-\overline{u'w'}$  component while the  $-\overline{u'v'}$  component shows the largest dispersion both in wintertime as well as in summertime. Furthermore, for larger wind velocities the obtained values of Reynolds shear stress do not meander as much as they do during the periods of smaller wind velocities. While the wind velocity in wintertime is larger than the velocity in summertime, the spread of values for all three Reynolds shear components on all three height level is larger in summertime than in wintertime. There is no distinctive day to night trend.

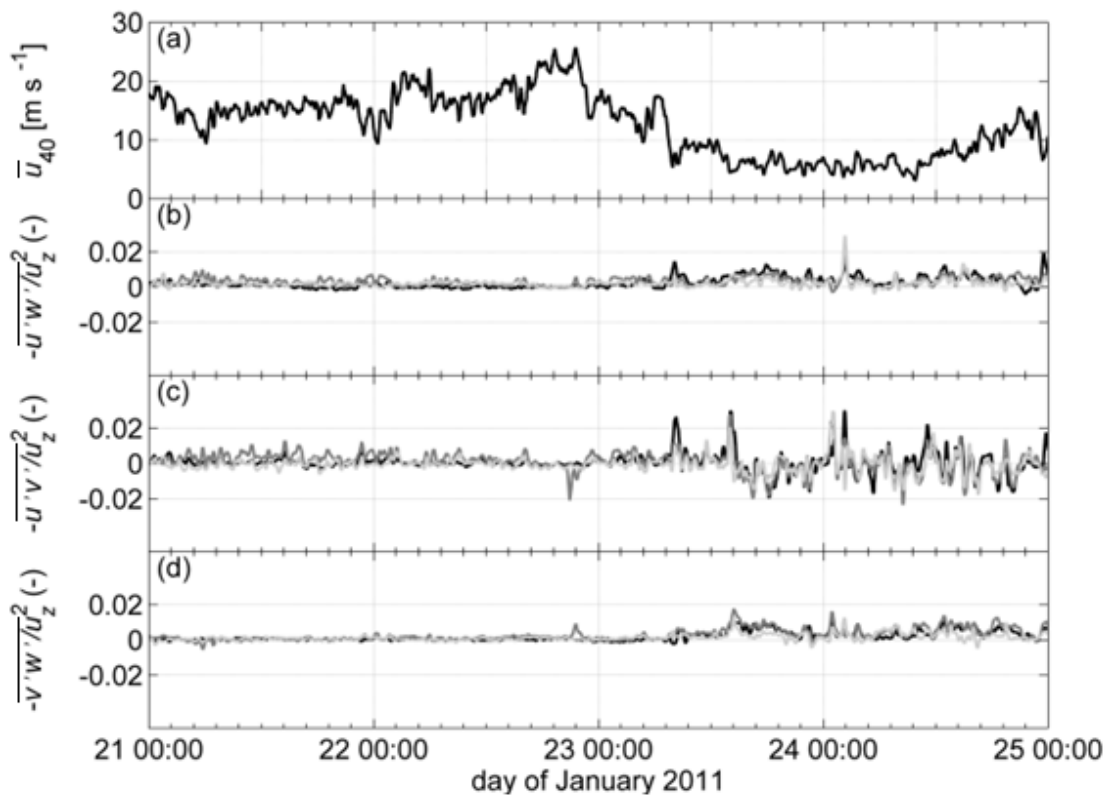


Fig. 15 Time series of (a) mean wind velocity in the main ( $x$ ) wind direction at 40 m height; time series of the calculated Reynolds shear stress components, (b)  $-\overline{u'w'}$ , (c)  $-\overline{u'v'}$  and (d)  $-\overline{v'w'}$  all normalized with the mean wind velocity squared in the main ( $x$ ) wind direction at corresponding height. Black curve is Reynolds shear stress at 10 m, dark gray curve is Reynolds shear stress at 22 m and light gray is Reynolds shear stress at 40 m height for the #12 summertime Bora episode

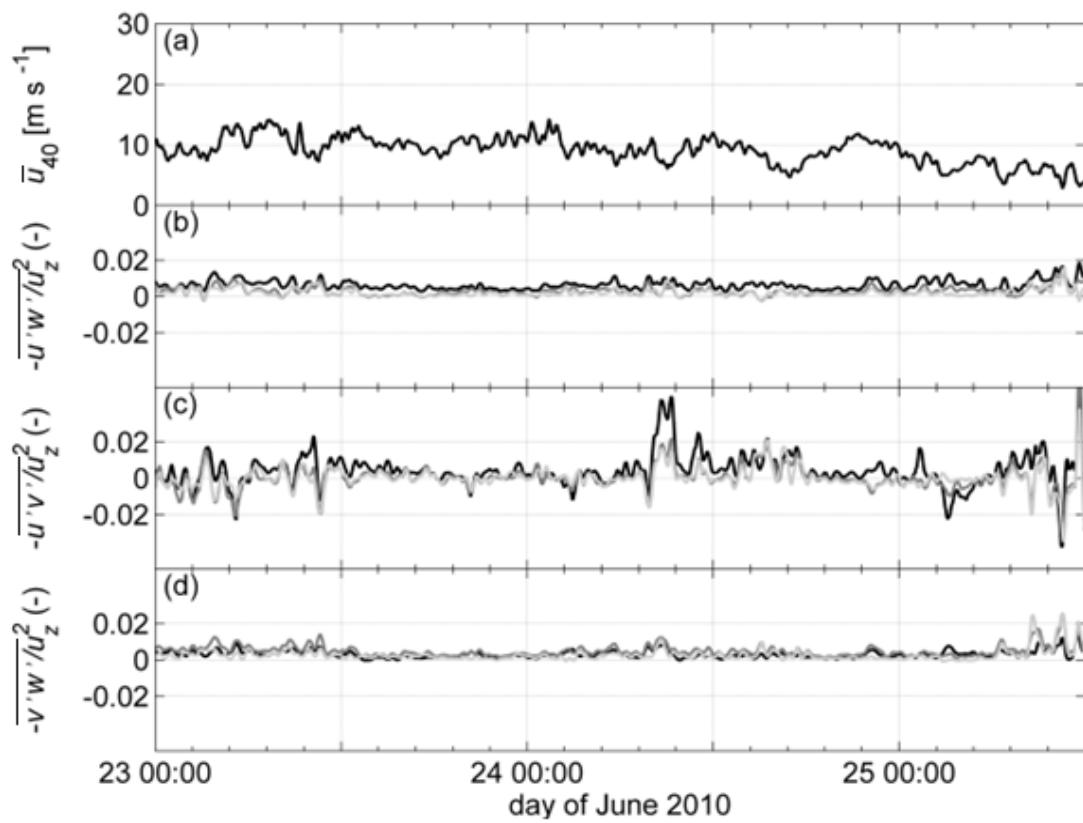


Fig. 16 Time series of (a) mean wind velocity in the main ( $x$ ) wind direction at 40 m height; time series of the calculated Reynolds shear stress components, (b)  $-\overline{u'w'}$ , (c)  $-\overline{u'v'}$  and (d)  $-\overline{v'w'}$  all normalized with the mean wind velocity squared in the main ( $x$ ) wind direction at corresponding height. Black curve is Reynolds shear stress at 10 m, dark gray curve is Reynolds shear stress at 22 m and light gray is Reynolds shear stress at 40 m for the #63 wintertime Bora episode

Figs. 17 and 18 display time series of turbulence length scales in the  $x$ -direction together with the mean wind velocity on all three measurement levels. Turbulence length scale component  ${}^xL_u$  has the largest values and  ${}^xL_w$  has the smallest values on all three height levels. The maximum values of  ${}^xL_u$  are around 300 m in summertime and well above 300 m in wintertime. The values are larger for larger wind velocities and smaller for smaller wind velocities. There is no day to night trend. This seasonal variability will be further analyzed more extensively in the future.

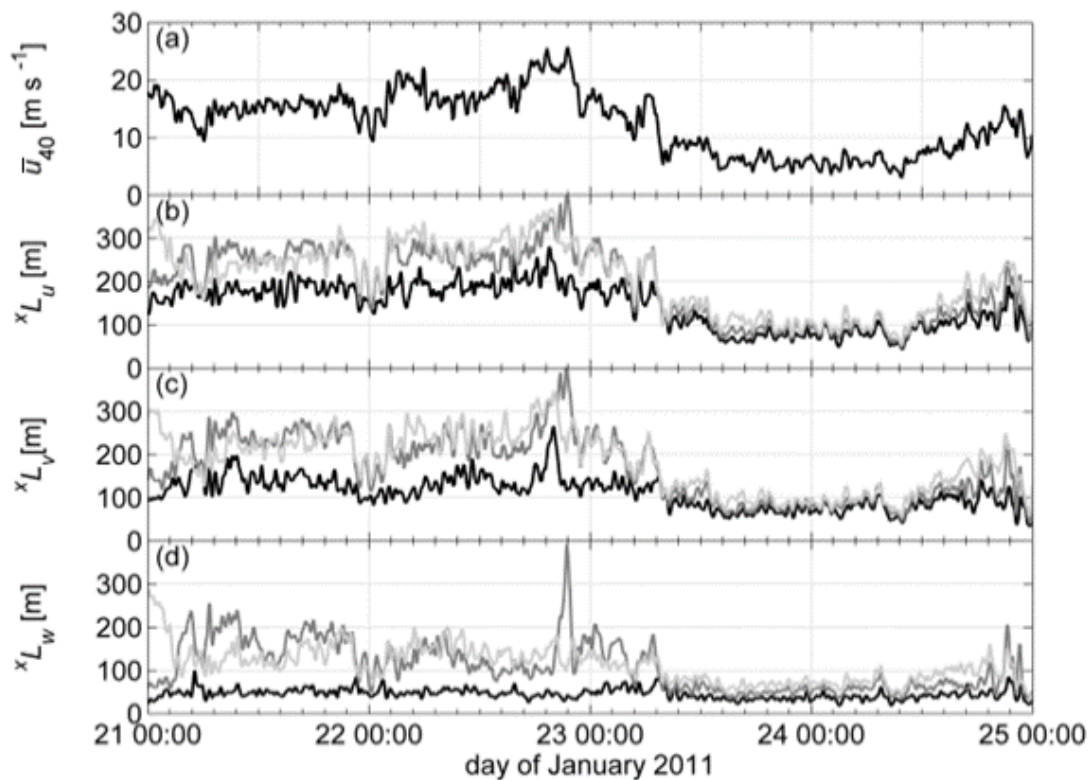


Fig. 17 Time series of (a) mean wind velocity in the main ( $x$ ) wind direction at 40 m height; time series of turbulence length scales, (b)  ${}^xL_u$ , (c)  ${}^xL_v$  and (d)  ${}^xL_w$ . Black curve are turbulence length scales at 10 m, dark gray curve are turbulence length scales at 22 m and light gray are turbulence length scales at 40 m height for the #24 summertime Bora episode

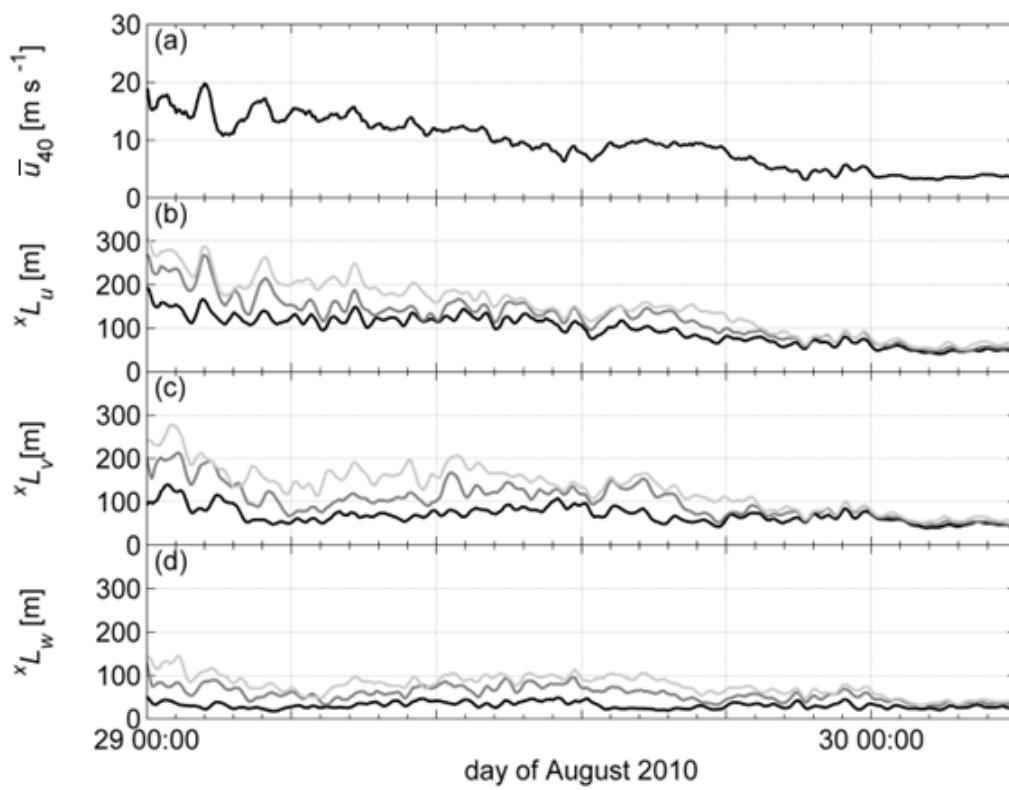


Fig. 18 Time series of (a) mean wind velocity in the main ( $x$ ) wind direction at 40 m height; time series of turbulence length scales, (b)  $^xL_u$ , (c)  $^xL_v$  and (d)  $^xL_w$ . Black curve are turbulence length scales at 10 m, dark gray curve are turbulence length scales at 22 m and light gray are turbulence length scales at 40 m height for the #63 wintertime Bora episode

The calculated mean values of thermal stability parameter for each Bora episode together with the fitted normal distribution are presented in Fig. 19. The Obukhov length is calculated separately for each Bora episode using the constant mean ultrasonic temperature and the turbulent heat flux calculated using this temperature. Since the mean values are close to zero, this indicates that the observed Bora episodes are near to a neutral thermal stratification.

In Figs. 20 and 21 the power spectral density of longitudinal, lateral and vertical Bora velocity fluctuations are presented for the #12 summertime and the #75 wintertime Bora episodes. Measurement results are compared with the power spectral density proposed in ESDU 85020 (1985), according to von Kármán (1948). In general, a spectral distribution of Bora turbulent kinetic energy (TKE) differs from the ESDU 85020 (1985) recommendation provided for the ABL. With respect to the classical bell shape, the obtained energy spectra show non typical behavior.

In particular, Bora TKE is distributed across a wider range of frequencies than ESDU 85020 (1985) values, Bora spectrum is more flat without a distinct peak, and there is a strong energy content at high frequencies. This applies to all three Bora velocity components on all three height levels. This is possibly due to the fact that the contribution of Bora wind to turbulence likely affects small scales stronger than the large scales, which is to be further investigated in more detail in the future at larger sampling rates than it is the case in the present study.

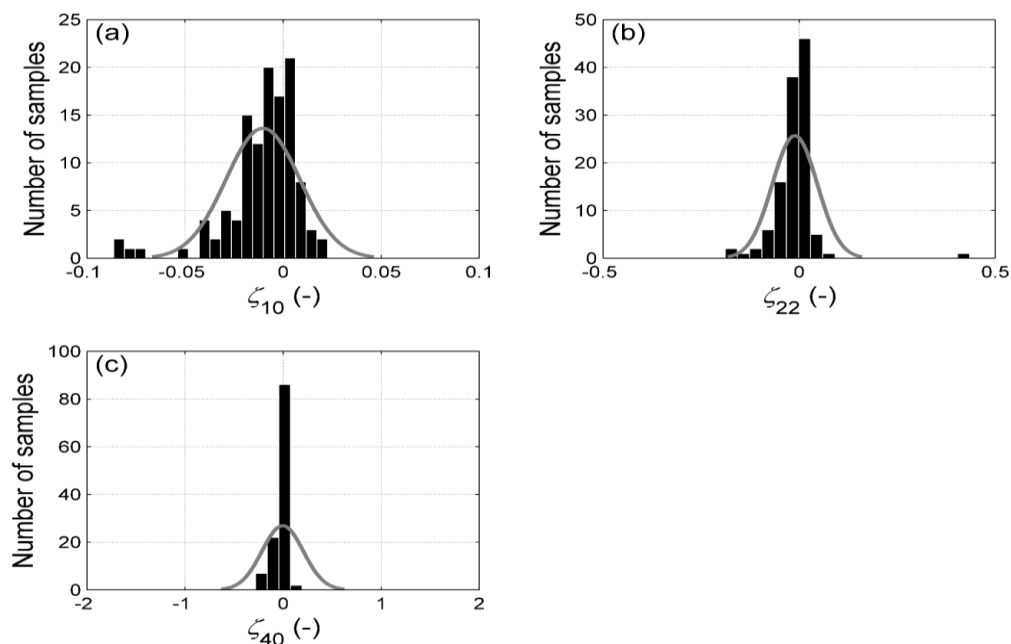


Fig. 19 Mean stability parameter with fitted normal distribution at (a) 10 m, (b) 22 m and (c) 40 m height

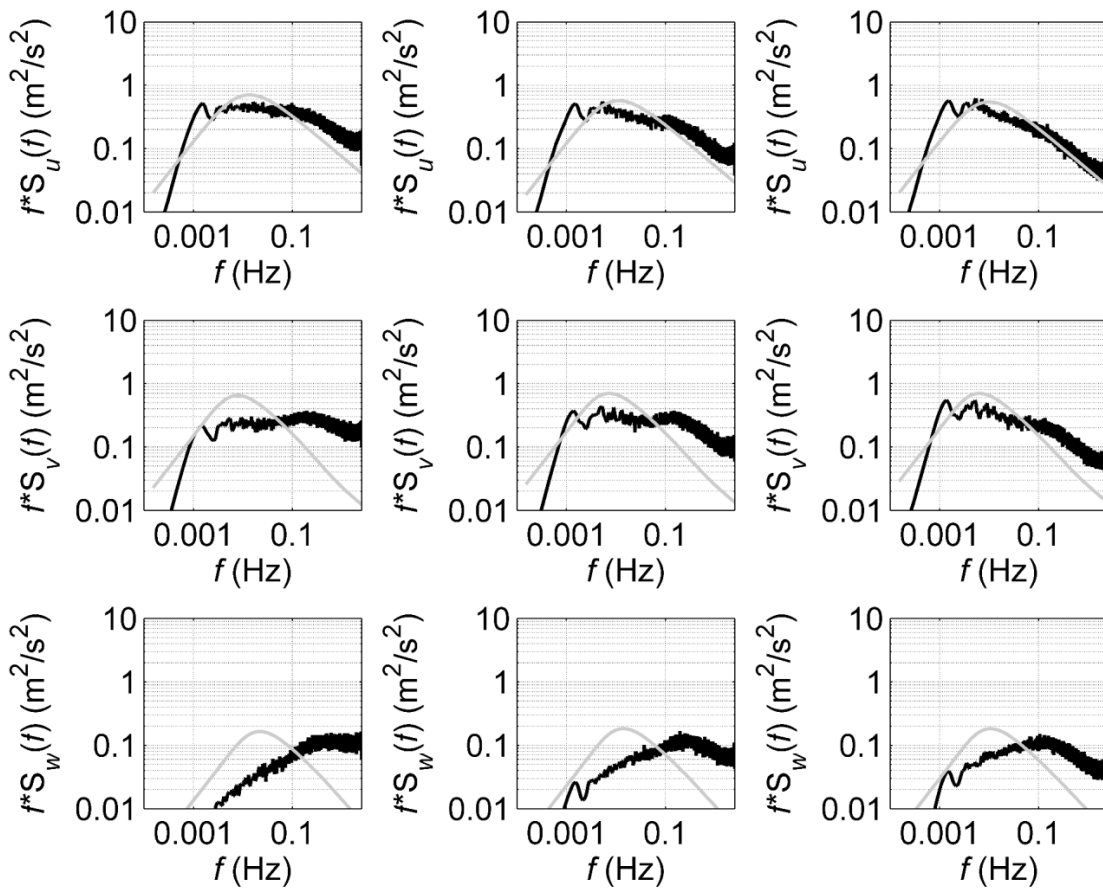


Fig. 20 Power spectral density of Bora velocity fluctuations compared with ESDU 85020 (1985). Legend: Black curve is power spectral density for the #12 summertime Bora episode. Grey curve is ESDU 85020 (1985). Left is power spectral density on 40 m, in the middle on 22 m and on the right on 10 m height

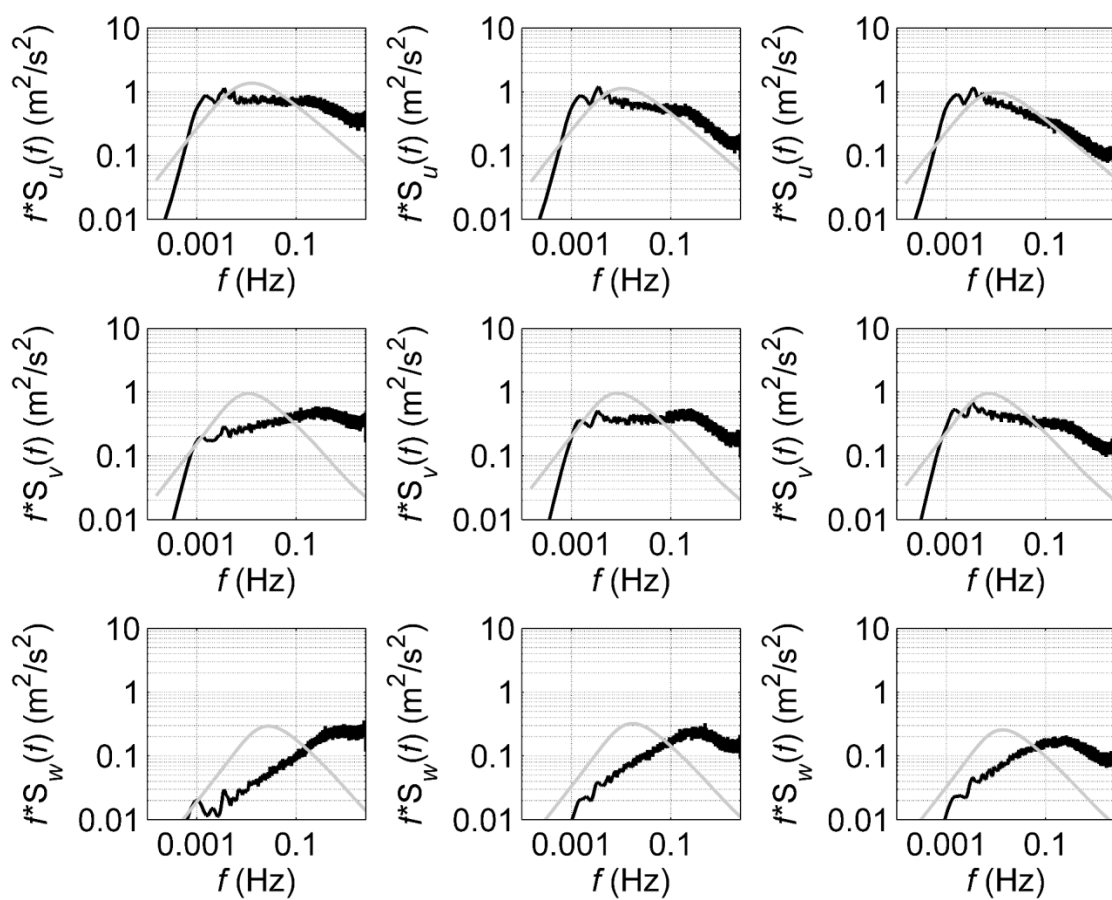


Fig. 21 Power spectral density of Bora velocity fluctuations compared with ESDU 85020 (1985). Legend: Black curve is power spectral density for the #75 wintertime Bora episode. Grey curve is ESDU 85020 (1985). Left is power spectral density on 40 m, in the middle on 22 m and on the right on 10 m height

#### 4. Conclusions

Bora wind velocity and near-ground turbulence are analyzed using the results of three-level high-frequency field measurements carried out on the meteorological tower close to the city of Split, Croatia, from April 2010 until June 2011. In total, 119 Bora episodes are analyzed. The studied parameters include the mean Bora wind velocity, turbulence intensity, Reynolds shear stress, turbulence length scales, velocity power spectra and thermal stratification. The important findings include the following conclusions:

- Bora is near-neutral thermally stratified. Differences in day to night trends are negligible. Bora has larger velocities and longer duration in wintertime than in summertime.
- Mean velocity profile in the main Bora direction agrees well with the power-law and logarithmic-law approximations. An increase in the power-law exponent and the aerodynamic surface roughness length and a decrease of the friction velocity with decreasing Bora mean wind velocity indicates rural-like velocity profile for larger wind velocities and an urban-like velocity profile for smaller velocities.
- Turbulence intensity generally agrees with ESDU 85020 (1985), unlike the turbulent Reynolds shear stress.
- Turbulence intensity and Reynolds shear stress remain nearly constant for mean velocities larger than 5 m/s. This indicates that 5 m/s can be considered as a critical velocity for the Bora wind.
- Turbulence length scales increase with increasing mean wind velocity and vice versa. Longitudinal component of turbulence length scale in the main (longitudinal) wind direction generally agrees well with standard values, while lateral and vertical components are much larger than in ESDU 85020 (1985).
- Spectral distribution of Bora turbulent kinetic energy differs from ESDU 85020 (1985), as it is distributed across a wider range of frequencies than ESDU 85020 (1985) values, Bora spectrum is more flat, without a distinct peak, and there is a strong energy content at high frequencies.

#### Acknowledgments

The authors acknowledge the Croatian Science Foundation IP-2016-06-2017 (WESLO) and the Meteorological and Hydrological Service support.

#### References

- Aboshosha, H. and El Damatty, A. (2015), "Dynamic response of transmission line conductors under downburst and synoptic winds", *Wind Struct.*, **21**(2), 241-272.
- Àgústsson, H. and Ólafsson, H. (2007), "Simulating a severe windstorm in complex terrain", *Meteorologische Zeitschrift*, **16**, 111-122.
- Babić, N., Večenaj, Ž., Kozmar, H., Horvath, K., De Wekker, S.F. and Grisogono, B. (2016), "On turbulent fluxes during strong winter bora wind events", *Bound. – Lay. Meteorol.*, **158**, 331-350.
- Belušić, D. and Klaić, Z.B. (2004), "Estimation of Bora wind gusts using a limited area model", *Tellus*, **56**,

- 296-307.
- Belušić, D. and Klaić, Z.B. (2006), "Mesoscale dynamics, structure and predictability of a severe Adriatic Bora case", *Meteorologische Zeitschrift*, **15**, 157-168.
- Belušić, D., Hrastinski, M., Večenaj, Ž. and Grisogono, B. (2013), "Wind regimes associated with a mountain gap at the northeastern Adriatic coast", *J. Appl. Meteorol. Clim.*, **52**, 2089-2105.
- Belušić, D., Pasarić, M. and Orlić, M. (2004), "Quasi-periodic bora gusts related to the structure of the troposphere", *Q. J. Roy. Meteor. Soc.*, **130**, 1103-1121.
- Belušić, D., Pasarić, M., Pasarić, Z., Orlić, M. and Grisogono, B. (2006), "A note on local and non-local properties of turbulence in the bora flow", *Meteorologische Zeitschrift*, **15**, 301-306.
- Belušić, D., Žagar, M. and Grisogono, B. (2007), "Numerical simulation of pulsations in the Bora wind", *Q. J. Roy. Meteor. Soc.*, **133**, 1371-1388.
- Cao, Y. and Fovell, R.G. (2016), "Downslope windstorms of San Diego county. Part I: A case study", *Mon. Weather Rev.*, **144**, 529-552.
- Counihan, J. (1975), "Adiabatic atmospheric boundary layers: a review and analysis of data from the period 1880-1972", *Atmos. Environ.*, **9**, 871-905.
- Enger, L. and Grisogono, B. (1998), "The response of bora-type flow to sea surface temperature", *Q. J. Roy. Meteor. Soc.*, **124**, 1227-1244.
- ESDU Data Item No. 74030. (1976), "Characteristics of atmospheric turbulence near the ground. Part I: definitions and general information", Engineering Science Data Unit, London, UK.
- ESDU Data Item No. 85020. (1985), "Characteristics of atmospheric turbulence near the ground. Part II: single point data for strong winds (neutral atmosphere)", Engineering Science Data Unit, London, UK.
- Grisogono, B. and Belušić, D. (2009), "A review of recent advances in understanding the meso- and micro-scale properties of the severe Bora wind", *Tellus*, **61**, 1-16.
- Grubišić, V. (2004), "Bora-driven potential vorticity banners over the Adriatic", *Q. J. Roy. Meteor. Soc.*, **130**, 2571-2603.
- Heimann, D. (2001), "A model-based wind climatology of the eastern Adriatic coast", *Meteorologische Zeitschrift*, **10**, 5-16.
- Hellman, G. (1916), "Über die Bewegung der Luft in den untersten Schichten der Atmosphäre", *Meteorologische Zeitschrift*, **34**, 273-285.
- Jackson, P.L., Mayr, G. and Vosper, S. (2013), "Dynamically-Driven Winds", (Eds., Chow F.K., De Wekker S.F.J. and Snyder B.J.), Mountain Weather Research and Forecasting. Recent Progress and Current Challenges, Springer, Dordrecht, Netherlands.
- Jurčec, V. (1981), "On mesoscale characteristics of Bora conditions in Yugoslavia", *Pure Appl. Geophys.*, **119**, 640-657.
- Jurčec, V. and Visković, S. (1994), "Mesoscale characteristics of southern Adriatic Bora storms", *Geofizika*, **11**, 33-46.
- Klemp, J.B. and Durran, D.R. (1987), "Numerical modelling of Bora winds", *Meteorol. Atmos. Phys.*, **36**, 215-227.
- Kozmar, H., Allori, D., Bartoli, G. and Borri, C. (2016), "Complex terrain effects on wake characteristics of a parked wind turbine", *Eng. Struct.*, **110**, 363-374.
- Kozmar, H., Butler, K. and Kareem A. (2015), "Downslope gusty wind loading of vehicles on bridges", *J. Bridge Eng.*, **20**(11), 04015008.
- Kozmar, H., Butler, K. and Kareem, A. (2012a), "Transient cross-wind aerodynamic loads on a generic vehicle due to bora gusts", *J. Wind Eng. Ind. Aerod.*, **111**, 73-84.
- Kozmar, H., Procino, L., Borsani, A. and Bartoli, G. (2012b), "Sheltering efficiency of wind barriers on bridges", *J. Wind Eng. Ind. Aerod.*, **107**, 274-284.
- Kozmar, H., Procino, L., Borsani, A. and Bartoli, G. (2014), "Optimizing height and porosity of roadway wind barriers for viaducts and bridges", *Eng. Struct.*, **81**, 49-61.
- Kuzmić, M., Grisogono, B., Li, X.M. and Lehner, S. (2015), "Discerning a deep and a shallow Adriatic bora event", *Q. J. Roy. Meteor. Soc.*, **141**, 3434-3438.
- Lepri, P., Kozmar, H., Večenaj, Ž. and Grisogono, B. (2014), "A summertime near-ground velocity profile of

- the Bora wind”, *Wind Struct.*, **19**(5), 505-522.
- Lepri, P., Večenaj, Ž., Kozmar, H. and Grisogono, B. (2015), “Near-ground turbulence of the Bora wind in summertime”, *J. Wind Eng. Ind. Aerod.*, **147**, 345-357.
- Lou, W.J., Wang, J.W., Chen, Y., Lv, Z.B. and Lu, M. (2016), “Effect of motion path of downburst on wind-induced conductor swing in transmission line”, *Wind Struct.*, **23**(3), 41-59.
- Magjarević, V., Večenaj, Ž., Horvath, K. and Grisogono, B. (2011), “Turbulence averaging interval for summer Bora flows at the middle of the NE Adriatic coast”, *Proceedings of the Poster, 31st International Conference on Alpine Meteorology*, Aviemore, Scotland, 23-27 May 2011.
- Makjanić, B. (1978), “Bura, jugo, etezija”, *Prilozi poznavanju vremena i klime u SFRJ*, **5**, 1-43.
- Neiman, P.J., Hardesty, R.M., Shapiro, M.A. and Cupp, R.E. (1988), “Doppler lidar observations of a downslope windstorm”, *Mon. Weather Rev.*, **116**, 2265-2275.
- Pandžić, K. (2002), “Analiza meteoroloških polja i sustava”, HINUS, Zagreb, Croatia.
- Papoulis, A. and Pillai, S.U. (2002), “Probability, Random Variables, and Stochastic Processes”, McGraw-Hill Europe.
- Petkovšek, Z. (1976), “Periodicity of Bora gusts”, *Rasprave-Papers SMD*, **20**, 67-75.
- Petkovšek, Z. (1982), “Gravity waves and Bora gusts”, *Annalen der Meteorologie*, **19**, 108-110.
- Petkovšek, Z. (1987), “Main Bora gusts - a model explanation”, *Geofizika*, **4**, 41-50.
- Poje, D. (1992), “Wind persistence in Croatia”, *Int. J. Climatol.*, **12**, 569-586.
- Rakovec, J. (1987), “Preliminary report on spectral characteristics of Bora on the island of Rab”, *Geofizika*, **4**, 35-40.
- Simiu, E. and Scanlan, R.H. (1996), “Wind effects on structures”, John Wiley, New York, NY, USA.
- Smith, R.B. (1987), “Aerial observations of Yugoslavian Bora”, *J. Atmos. Sci.*, **44**, 269-297.
- Solari, G. (2014), “Emerging issues and new frameworks for wind loading on structures in mixed climates”, *Wind Struct.*, **19**(3), 295-320.
- Solari, G., Burlando, M., De Gaetano, P. and Repetto, M.P. (2015), “Characteristics of thunderstorms relevant to the wind loading of structures”, *Wind Struct.*, **20**(6), 763-791.
- Stull, R.B. (1988), “An introduction to boundary layer meteorology”, Kluwer, Dordrecht, Netherlands.
- Thuillier, R.H. and Lappe, U.O. (1964), “Wind and temperature profile characteristics from observations on a 1400 ft tower”, *J. Appl. Meteorol. Clim.*, **3**, 299-306.
- Večenaj, Ž., Belušić, D. and Grisogono, B. (2010), “Characteristics of the near-surface turbulence during a bora event”, *Ann. Geophys.*, **28**, 155-163.
- von Kármán, T. (1948), “Progress in the statistical theory of turbulence”, *Proceedings of the National Academy of Sciences*, **34**(11), 530-539.
- Yang, F.L. and Zhang, H.J. (2016), “Two case studies on structural analysis of transmission towers under downburst”, *Wind Struct.*, **22**(6), 685-701.